AD-A085 992 ITEK CORP LEXINGTON MASS OPTICAL SYSTEMS DIV F/G 17/8
RESEARCH AND DESIGN OF PROM COHERENT OPTICAL PROCESSOR.(U)
APR 80 F J CORBETT, R A TUFT, W FACCENDA DAAK70-79-C-0164
UNCLASSIFIED ITEK-9565-62 ETL-0219 NL

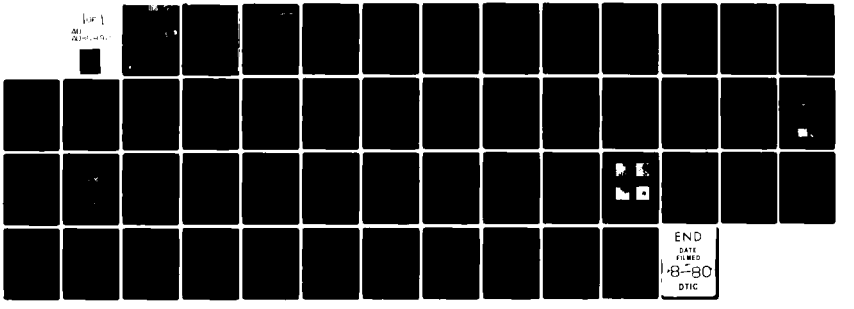

END
DATE FILMED
8-80
DTIC

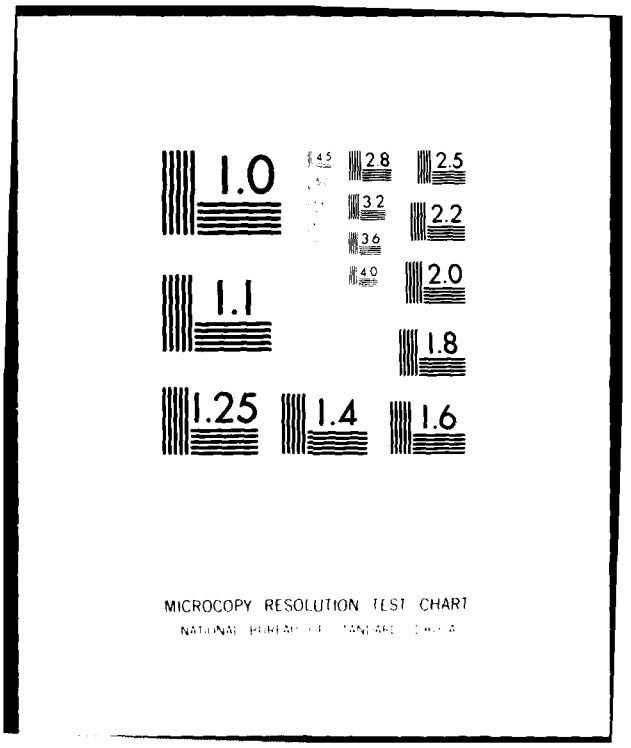
1.0
1.1
1.25
1.4
1.6
1.8
2.0
2.2
2.5
2.8
3.2
3.6
4.0
4.5
MICROCOPY RESOLUTION TEST CHART

ETL-0219

RESEARCH AND DESIGN OF A PRISM CORRELATOR OPTICAL PROCESSOR

Itek Corporation
Optical Systems Division
10 Maguire Road
Lexington, Massachusetts 02173

April 10, 1980

Final Report for September, 1979 - March, 1980

Approved for public release; distribution unlimited

Prepared for
U.S. ARMY ENGINEER TOPOGRAPHIC LABORATORIES
Ft. Belvoir, Virginia 22060

Destroy this report when no longer needed.
Do not return it to the originator.

The findings in this report are not to be construed as an official Department of the Army position unless so designated by other authorized documents.

The citation in this report of trade names of commercially available products does not constitute official endorsement or approval of the use of such products.

Preface

This document describes the program performed under Contract No. DAAK 70-79-C-0164 by Itek Corporation, Optical Systems Division, Lexington, Massachusetts, for the U.S. Army Engineer Topographic Laboratories (USAETL). The purpose of the work was to produce a design for the PROM Coherent Optical Processor (PCOP). The PCOP is a subsystem of the USAETL Hybrid (Optical/Digital) Image Processor which consists of the optical system to perform Fourier plane filtering (PCOP), a digital control and feedback system, and a graphic display for interactive operation. This system is to be used as a test bed processor for the development of automated image feature extraction algorithms. Design details and the supporting analysis are discussed in this report. This work was conducted between September 25, 1979 and March 7, 1980. Mr. John Benton was the USAETL Contracting Officer's Technical Representative. The contractor wishes to thank Mr. Benton, Mr. Michael McDonnell, and Mr. Robert Leighty for their guidance.

SECURITY CLASSIFICATION OF THIS PAGE (When Data Entered)

REPORT DOCUMENTATION PAGE

READ INSTRUCTIONS BEFORE COMPLETING FORM

1. REPORT NUMBER: ETL-0219	2. GOVT ACCESSION NO.: AD-A085992
3. RECIPIENT'S CATALOG NUMBER	
4. TITLE (and Subtitle): Research and Design of A PROM Coherent Optical Processor.	5. TYPE OF REPORT & PERIOD COVERED: Final Technical Report. Sept 25, 1979 — March [illegible] 1980
	6. PERFORMING ORG. REPORT NUMBER: 9565-62
7. AUTHOR(s): Francis J. Corbett, Richard A. Tuft, W. Faccenda, R. Cooper, A. Rux	8. CONTRACT OR GRANT NUMBER(s): DAAK 70-79-C-0164
9. PERFORMING ORGANIZATION NAME AND ADDRESS: Itek Corporation, Optical Systems Division, 10 Maguire Road, Lexington, Massachusetts 02173	10. PROGRAM ELEMENT, PROJECT, TASK AREA & WORK UNIT NUMBERS
11. CONTROLLING OFFICE NAME AND ADDRESS: U.S. Army Engineer Topographic Laboratories, Research Institute, Fort Belvoir, Virginia 22060	12. REPORT DATE: 10 Apr [illegible] 80 13. NUMBER OF PAGES
14. MONITORING AGENCY NAME & ADDRESS (if different from Controlling Office)	15. SECURITY CLASS. (of this report): Unclassified 15a. DECLASSIFICATION/DOWNGRADING SCHEDULE

16. DISTRIBUTION STATEMENT (of this Report)

Approved for public release; distribution unlimited

17. DISTRIBUTION STATEMENT (of the abstract entered in Block 20, if different from Report)

ITEK-9565-62

18. SUPPLEMENTARY NOTES

A summary of the ETL Hybrid (Optical/Digital) Image Processor design details is also published in SPIE Vol. 218, "Devices and Systems for Optical Signal Processing," May, 1980.

19. KEY WORDS (Continue on reverse side if necessary and identify by block number)

Hybrid Image Processing; Optical Processing; PROM (Pockels Readout Optical Modulator); Electro-Optics; Coherent Optics; Pattern Recognition; Automatic Feature Extraction; Algorithm Development

20. ABSTRACT (Continue on reverse side if necessary and identify by block number)

This program produced a design for a coherent optical image processor utilizing a PROM(s). The PROM Coherent Optical Processor or PCOP is a subsystem of the USAETL Hybrid (Optical/Digital) Image Processor. The design and supporting analysis tasks are detailed in the report. The purpose of development of this processor is to evaluate automatic image feature extraction algorithms.

(continued)

DD FORM 1 JAN 73 1473 EDITION OF 1 NOV 65 IS OBSOLETE

Unclassified

SECURITY CLASSIFICATION OF THIS PAGE (When Data Entered)

404157

The PCOP is a two PROM Fourier plane filter processor which operates in the following manner. The first PROM is the input image plane. Imagery is scaled through a lens system and then manipulated in intensity space at the input PROM. The image transform is taken next in the processing sequence and then filtered at the second PROM. Filters are generated with a laser optical scanner. The reconstructed image is produced on a charge integrating camera and displayed on a CRT.

The system functions interactively. An operator will control the PROM, filtering, and display parameters with the goal of optimizing the feature extraction process.

This design is unique in the following ways: First, the optical imaging and filtering operations have been made compatible with the frequency response of the PROM; and second, Fourier filtering is implemented by generation of the appropriate pattern with the laser optical scanner and then with rotation of the filter medium or PROM, as opposed to rotation of the data with respect to a stationery filter.

Image quality and data throughput were determined and the PCOP design was made to insure the output quality was compatible with the USAETL program objectives.

TABLE OF CONTENTS

TABLE OF CONTENTS

(continued)

FIGURES

FIGURES

(Continued)

TABLE OF TABLES

1. INTRODUCTION AND PROGRAM STRUCTURE

The PROM Coherent Optical Processor (PCOP) is the optical subsystem of the Hybrid Processor currently under development at USAETL. Within this program, the PCOP system concept was analyzed and modified where appropriate. A final design was produced which incorporated both off-the-shelf and specially designed hardware.

Because of USAETL's intention to build this test bed image processor by utilizing existing hardware where possible, and to capitalize on their previous experience and investments, the design has incorporated both their efforts and equipment. Consequently, the program was structured to facilitate a close working relationship with USAETL.

Work was performed in three categories: Analysis, Design Engineering, and PROM Electronics Hardware.

The analysis task evaluated the hybrid digital-optical image processing concept developed by USAETL. Important functions were identified, and trade-offs were performed to establish optimum modes of operation.

The Design Engineering task took the image processing system from a schematic stage to layout and assembly drawings compatible with the mixture of existing, purchased, and specially designed hardware. Much of the initial program effort was directed at insuring the efficient use of customer furnished equipment (CFE) as well as interfacing the complementary analytical tasks performed both by USAETL and Itek.

Modified PROM electronics hardware, designed to be compatible with the USAETL system controller, was built and tested under a separate task of the program.

2. SUMMARY OF THE PROGRAM

2.1 PROM Coherent Optical Processor Description

The PCOP system specification required that the optical processor operate in two distinct modes.

In its primary operating mode, the PCOP is used as a two PROM processor designed to perform both intensity operations at the input image plane and PROM and spatial filtering at the Fourier plane PROM. The system will operate on an aerial image transparency as input and produce a reconstructed image at the output. This concept is illustrated in Figure 2.1

In the secondary mode, the image plane PROM and relay optics are absent. The input transparency is coherently illuminated, and spatial filtering is performed at the filter plane PROM.

Fig. 2.1 - PROM Coherent Optical Processor General Schematic

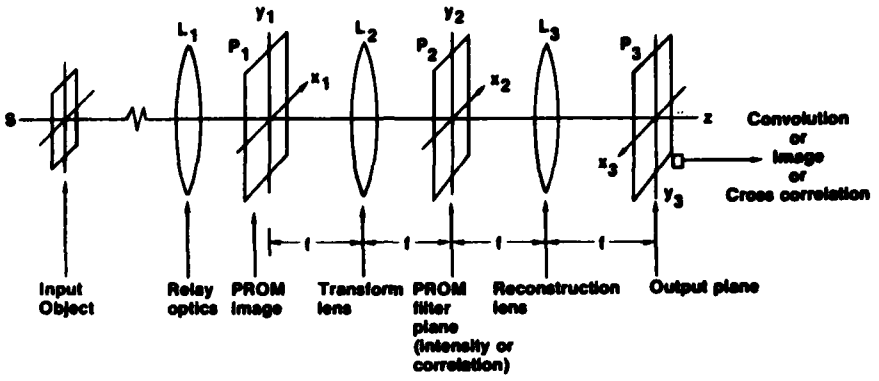

The hybrid processor is a coherent optical Fourier image processor which allows the option of producing either a reconstructed, filtered image or image correlation, depending on the type of filter used. Both the incoherent input imaging system and the coherent Fourier filtering system were designed to optimize the performance of the PROM. Processing operations at the first PROM will include contrast enhancement and coherent noise suppression with the first PROM performing the function of a liquid gate. Once the spatial frequency content of the input imagery is made similar to the range of appreciable PROM response by a zoom lens, the input PROM image will become the input to a conventional coherent Fourier Processor. Lens L_2 of Figure 2.1 is the Fourier transform lens. PROM Baseline Subtraction[1] can be used to adjust the image intensity and suppress the D.C. in the Fourier Transform. A Fourier plane filter, written on the Filter PROM by a laser scanner, will effect the desired filtering operation. The image is then reconstructed onto a CID sensor or film for display. Interactive feedback is facilitated for image/filter optimization. The integrated transform is sensed and interpreted for further analysis by the control electronic system.

2.2 Analysis

Figure 2.2 is a block diagram of the PROM Coherent Optical Processor Analysis which shows major tasks and results. It illustrates the image processor's three basic functions: Input Imaging; Transforming and Filtering; and Reconstruction. The block diagram shows the hierarchy of work and the tasks performed for each subsystem. Details of these tasks will be described in Section 4.

Fig. 2.2 - PROM Coherent Optical Processor Analysis

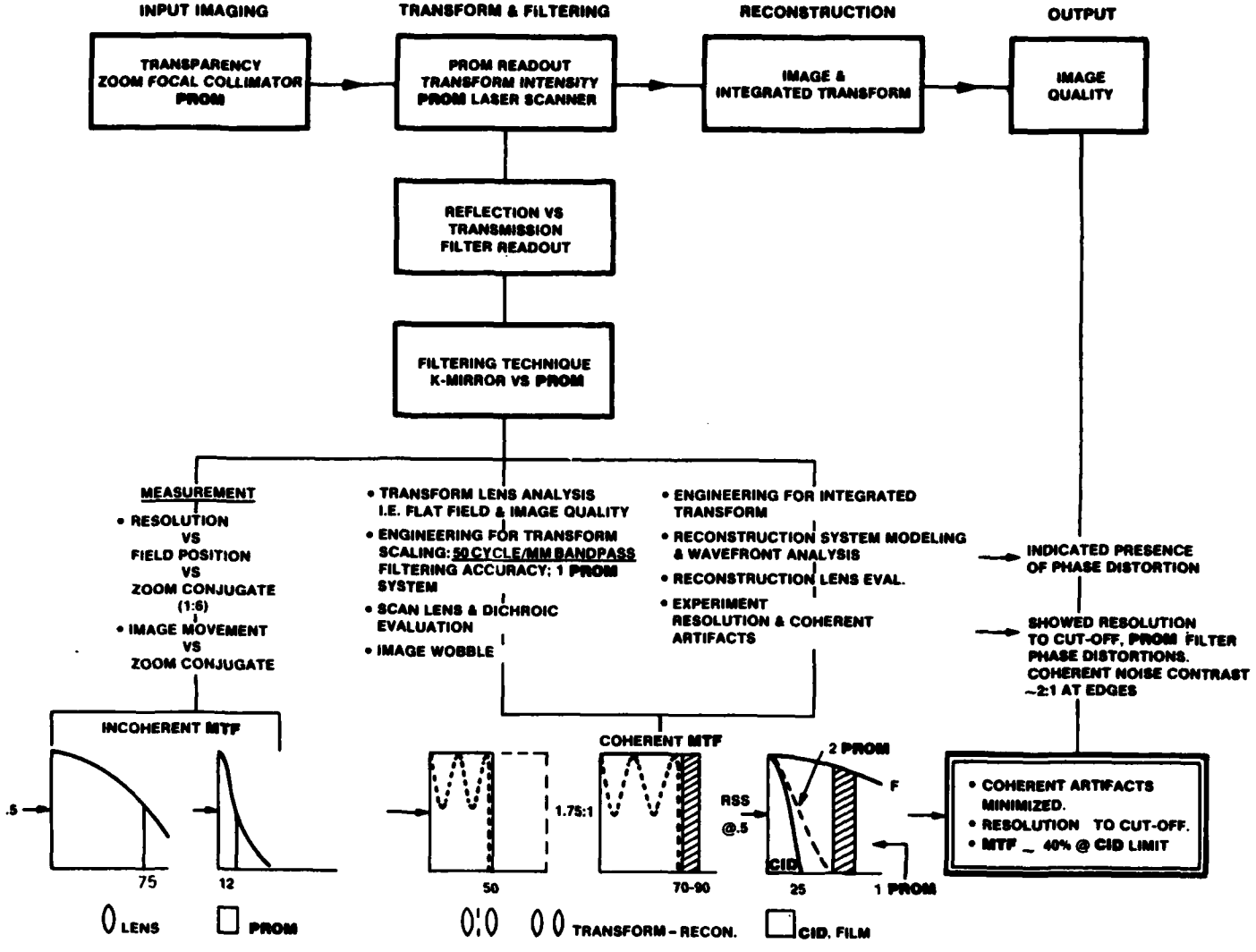

The USAETL hybrid image processing concept is based on the need for a test bed to develop algorithms for rapid automatic feature extraction utilizing the PROM spatial light modulator as an interactively controlled Fourier plane filter. Previous experience has shown some success with feature extraction by Fourier plane filtering. To bring this technique to a more mature state of development, however, a real-time interactive system is required.

The Input Imaging subsystem has to be compatible with the need to operate on aerial imagery transparencies and the need for a transitional image plane into the processor. The input system must facilitate the transition from relatively high spatial frequency input imagery to the lower frequency response of the spatial light modulator and, in addition, must be compatible with the spatial frequency range found most useful for image data extraction. The Transform and Filtering subsystem is designed to be compatible with the USAETL PROM Laser Scanner and with the use of the PROM as the filter medium. These and the Reconstruction subsystem, in particular, are optimized with respect to the required output for an integrated transform and a filtered image recorded on a CID camera; both functions are necessary for the feedback optimization and final image interpretation.

The initial analysis, as shown in Figure 2.2, was performed to address the following two items:

A) The optimum method of Filter PROM Readout (in reflection or transmission)

B) The Filtering Technique

PROM's have been addressed for readout both by reflection and transmission in the past. Because each mode has certain advantages and disadvantages, and because the selection of readout mode impacts on the optical architecture, this analysis was performed first.

The image filtering technique also affects the optical system design. The PROM Laser Scanner (PLS), built by USAETL, is the mechanism by which various intensity blocking filters will be generated on the Fourier plane PROM, and thus is the mechanism for varying the filter parameters. In image pattern recognition, there exists a well known relationship between angular orientation in the Fourier spectrum and structure in the image. This relationship can be exploited in feature extraction studies. Consequently, the ability to rotate the filter with respect to the image was required by USAETL. This analysis became a trade-off between rotating the image with a K-Mirror and rotating the filter.

Once tasks A and B were completed, we were able to perform the detailed analysis and optical design. The end result was an image processor with the following capabilities.

2.3 PROM Coherent Optical Processor Capabilities

TWO PROM SYSTEM

- Input transparencies are imaged at conjugates varying over the range 1:6 onto the input PROM with insignificant loss of resolution through the imaging system (see results in Figure 2.2 and Section 4.4). Zoom and focus are presently accomplished manually with future updating expected to produce automatic drive.*

*While full automatic drive and computer control for all optical operations was initially desired by USAETL, it was agreed that manual control would be more suited for the initial use intended for the Hybrid Image Processor.

- Input image diameter: 3 mm < d < 19 mm (for simultaneous processing). However, the input image plane accommodates up to a 4" x 5" transparency and provides x, y, z translations (motor driven) over the desired range.

- Image plane processing is performed on the input PROM device via standard PROM intensity function variables. (See references 1, 2, 3).

- Focus on the first PROM is facilitated with a removable microscope viewing device.

- A Fourier transform of the image is performed and spatial processing is performed by filtering the aerial transform. This filter is generated by the PLS. The upper cutoff frequency of the filter is 40 to 50 cycles/mm. The filter is rotated with respect to the transform spectrum by rotation of the PROM filter medium at a maximum rate of 67 degrees per second, through any angle up to and greater than 180°.

- The transform-reconstruction optical system produces an image whose modulation at the CID detector exceeds the CID modulation transfer function. The output image has approximately 40% modulation at the CID cutoff.

- A chopper mirror and secondary lens assembly produce an image of the transform onto a sensor coupled to the electronic control hardware.

- Processed image throughput rate is a function of: PROM exposure time (both input and filter), filter rotation time, and interactive feedback time. No specifications exist, partly due to the intended test bed application, but this time could eventually be $\geq$ 1 image/second.

The two PROM system is considered the primary processing mode. However, a one PROM image processor is also accommodated in the design. Both optical layouts are presented in the production drawings and the first system is illustrated in Figure 4.1. Details of the work which led to the final design are discussed in Section 4. The system will operate with the following capabilities:

ONE PROM SYSTEM

- The optical transforming - reconstruction system will remain the same.

- The input transparency is read out directly with the HeNe laser beam. The input PROM is removed for this operation, and the zoom optics are bypassed.

- Transform scale changes will be performed by placement of the transparency in the focusing beam between the transform lens and the Fourier plane PROM. The scale change will be accomplished by sliding the transparency in this beam. Transform scale change will be > 3:1.

- The reconstructed image conjugates will be set manually.

- As noted in Figure 2.2, output image quality will be potentially improved with the output spatial frequency limit now imposed by the Fourier band pass filter, and not the image PROM.

In summary, the image quality at the output has been made consistent with the USAETL requirements as noted in the Purchase Description, and the PROM Coherent Optical Processor performs the range of functions expected. Quality at the output is PROM/CID limited when either of these components is used at an image plane; image conjugates are compatible with the CID pixel size, and output quality for the one-PROM system is consistent with its off-the-shelf optical system quality.

2.4 Design Engineering

Detailed definition of components began upon completion of both the analysis and a schematic of the PROM Coherent Optical Processor. Dimensions were defined and adjustments made to insure a fit for all parts and subsystems.

The major assemblies of components are itemized below. They are titled here as in Figure 2.2 and can be found on the itemized parts lists referenced in the next section.

1. Input Imaging System
   - Incoherent Light Source and Accessories (HG Arc)
   - Input Object Positioning Stage with motor drive.
   - Zoom-Focal Collimator Assembly (including mounts)
     - Nikon 50-300 focal length zoom lens
     - Aero - Ektar 300 mm focal length lens
   - Dichroic Beamsplitter
   - Input PROM assembly

2. Transform and Filtering System
   - HeNe Laser and Accessories and beam expanding optics
   - Transform lens (Buhl triplet, 355 mm focal length)
   - Rotating Filter PROM Assembly with drive
     (PROM and 2 $\lambda/4$ plates and polarizers)
   - Dichroic Beamsplitter and Mount

3. Reconstruction System
   - Reconstruction Lens and Mount
     (El Nikkor, F:5.6, 240 mm focal length)
   - Chopper mirror, optics and detector for transform imaging
   - CID Camera and Display

This spatial filtering subsystem did not initially include the scan lens by which a filter is generated on the PROM. The final design, however, required that a new scan lens be specified because of the need to read out the filter PROM in transmission. This lens, a Tropel telecentric scan lens of 76.5 mm focal length, corrected for λ = 442 mm, has been previously specified, recommended, and subsequently purchased by ETL for this system. It is noted on the schematic and is item number 46 of the parts list.

2.4.1 Drawings and Parts List

The PCOP drawings and parts list were delivered under separate cover from the final report. They are detailed prints and a listing of all PCOP parts. The system can be purchased, manufactured, and assembled from them. All items delivered in this package are summarized in Table 2.1.

2.4.2 Interface Provisions

By mutual agreement between USAETL and Itek, the main effort on this program was to be directed at the PCOP Optical System Design. Those elements of the design which incorporated an electronic or electro-mechanical interface to the system computer were to be so designed that the interface could be easily accomplished by USAETL. In the final system design, the main points of interface were the following: the stepper driven x, y, input transparency holder, stepper driven PROM rotation mount, and PROM control Electronics. Where possible, the electro-mechanical interface was facilitated by the specification of UNISLIDE stepper driven slides, for which USAETL has already designed computer controlled drives. A new PROM electronics box, configured to allow flexible modes of external control, was constructed under this program and is described in Section 2.5.

The electronic interface between the system computer, the CID camera, and integrated transform detector is to be performed by USAETL.

2.5 PROM Electronics Hardware

The proper operation of the PCOP calls for external control of the PROM cycle. In response to this need, Itek produced a modified S1-210 PROM Control Electronics Box under this contract.

This box is now designated S1-210A. Its operational characteristics are described below. The circuit diagram for the S1-210A PROM box has also been delivered under separate cover.

In the preliminary design phase of the program, the operational characteristics of the modified PROM Box were defined by USAETL - Itek interaction and communicated to USAETL in a letter dated October 19, 1979. The required design changes did not increase the component count of the S1-210A.

As the design work progressed, it became clear that the modified PROM box could provide better external control interfaces by the addition of one CMOS integrated circuit at no additional cost to the program. The operation in this case differs from that outlined in the October 19 letter.

The S1-210A PROM box, as finally configured for this program, allows for either manual or externally triggered initiation of the PROM cycle with the following manually set timing ranges:

Erase: Preset at 3.5 msec

Record: 80 ms - 4 sec., by 10 turn pot

Readout: 80 ms - 4 sec., by 10 turn pot

Table 2.1

Design Drawings and Parts List Produced*
for the PROM Coherent Optical Processor

Title and Number	No. of Drawings & (Details)	No. of Fabricated Components	No. of+ Purchased Parts	No. of+ C.F.E. Items
1. Input Stage Assembly Film Holder; X,Y,Z (includes separate parts list) (198069)	2 (20)	29	3	
2. PROM Rotation Assembly (includes separate parts list) (198068)	1 (12)	22	5	1
3. Aero-Ektar Lens Mount Assembly (198070)	1	5		0
4. Image Plane Position #2 (for 1 PROM System) (198071)	1	2	1	
5. Mount-Zoom Lens (198074)	1	5		0
6. Mount Assembly Reconstruction Lens (198073)	1	5		1
7. Chopper Mirror Assembly (198111)	1	5	2	
8. Mount Assembly for Input PROM & Transform Lens (198072)	1 (6)	7		2
9. PROM Assembly (199943)	1			1
10. PROM Flash Box (211548)	1			1
11. PROM Coherent Optical Processor Layout and Parts List (198067)	1		109	6
TOTAL	12 (38)	80	120	12

*Items 9 and 10 relate to the PROM and are included in this package.

+The exact number of items available CFE for the PCOP was not established down to the basic component level. However, the system was designed to be compatible with the type of accessories used by ETL, and if some of these elementary parts, e.g., bases, mounts, and holders are available at the time of assembly, then the total number of purchased parts should be reduced.

Itek has facilitated external control of the S1-210A PROM Box by adding INTERNAL/EXTERNAL switches and BNC inputs to allow separate external triggers to the record and readout timers. In addition, an external input allows control of the baseline subtraction voltage by an externally controlled voltage ranging from 0 to +15 volts.

With all switches in the external mode, a +15V CMOS compatible pulse to the EXT TRIG IN will initiate the erase cycle. At the completion of ERASE, an ERASE SYNC OUT PULSE will be output, and the PROM voltage will then switch from erase voltage to record voltage. The record PROM voltage will be maintained irrespective of any input to the RECORD EXTERNAL TRIGGER. Assertion of the RECORD EXT. TRIG. will result in a positive RECORD TIME OUT Pulse which, together with the PROM Record voltage, will be maintained until a READOUT EXT. TRIG pulse occurs, irrespective of the status of the time set by the 10 turn pot. The READOUT EXT. TRIG. Pulse switches the PROM voltage to the preset baseline subtraction voltage and also initiates the READOUT TIME OUT Pulse. These levels will be maintained until another EXT. TRIG. initiates the ERASE Cycle. Figure 2.3 is a timing diagram for the totally external triggered case.

The time set by a particular 10 turn pot becomes operative when the subsequent timing function is internally triggered. As an example, if the ERASE and RECORD modes are externally triggered, and the READOUT mode is internally triggered, the RECORD TIME OUT is set by the 10 turn pot while the READOUT TIME OUT goes positive at the completion of the RECORD time and remains positive until an external trigger. Figure 2.4 is a timing diagram for the case of EXT. or MAN. TRIG for ERASE and INT. TRIG for RECORD and READOUT.

The modes of operation detailed here allow the driving of the various shutters in the system by RECORD and READOUT time out pulses whose durations are set by either the internally or externally controlled cycle times.

2.6 Deliverables

The following items are to be delivered to USAETL under this contract:

- PCOP Design Package including drawings (layouts and details), and comprehensive parts list.
- Final Report in which the analysis and justification for the design is presented.
- PROM S1-210A electronic control box.

TIMING DIAGRAM FOR MODIFIED S1-210A PROM ELECTRONICS

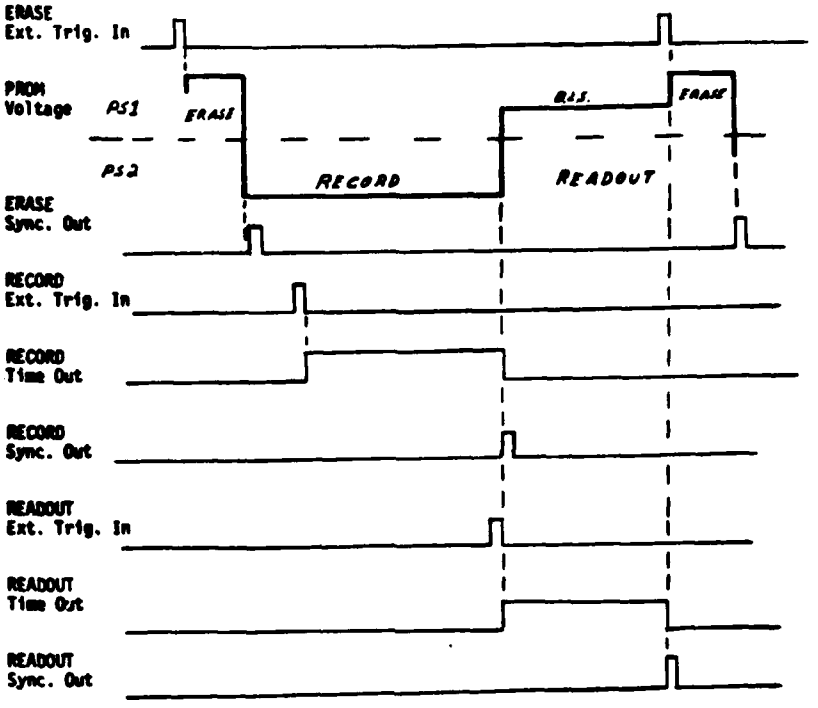

Fig. 2.3 - Ext. Trig. Mode for ERASE, RECORD and READOUT

TIMING DIAGRAM FOR MODIFIED S1-210A PROM ELECTRONICS

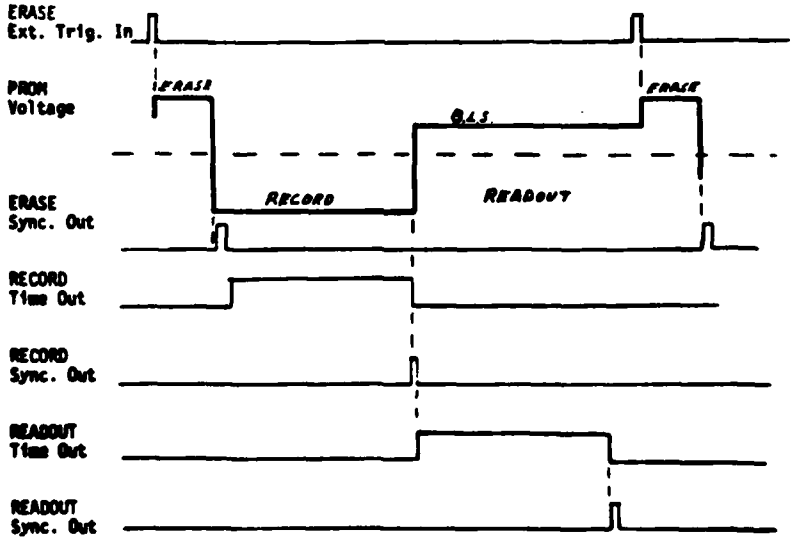

Fig. 2.4 - Ext. Trig. Mode for ERASE. Internal Trig. for RECORD and READOUT.

3.0 PROM OPERATION AND CHARACTERISTICS

The PROM is a single $Bi_{12}SiO_{20}$ crystal which is optically polished, covered with an insulator and then coated with transparent electrodes in order to maintain a voltage across the crystal.

The crystal is photo conductive when exposed to blue light. If an image is cast on a PROM in blue light, the image will be stored as a spatially varying potential distribution. Figure 3.1 illustrates the voltage across the insulating layers and the crystal at various phases of the PROM cycle. This spatially varying potential produces a pattern of birefringence in the crystal, through the Pockels effect, which is related to the original optical image of the PROM. This "Birefringent image" can be read out by means of a polarized light beam. If the readout beam is in the red region of the spectrum, image decay due to photo conductivity is minimized.

In the conventional method of PROM readout, the readout beam has a linear state of polarization. The PROM is oriented with its axes of birefringence oriented at 45^0 to the incoming plane of polarization, as shown in Figure 4.3(a). The birefringence, which is created by a stored charge image via the Pockels effect, results in an elliptical state of Polarization at the output of the PROM. The elliptical state of polarization results in an intensity modulation upon passage through a linear analyzer. The functional relationship between the throughput intensity and the voltage across the PROM takes the form,

$$I = I_o \sin^2 (kV),$$

where: I = throughput intensity

I_o = incident intensity

V = voltage across PROM

and k is the coefficient of the linear electro-optical, or Pockels, effect which relates the differential phase change through the PROM crystal, between orthogonal states of polarization, to the voltage across the crystal.

Modulation Transfer Functions for several PROM exposures are presented in Figure 3.2. These MTF's are typical of those obtained with any specific PROM.

Fig. 3.1 - PROM Operation

The Basic Steps and Voltage Cycle for PROM Operation

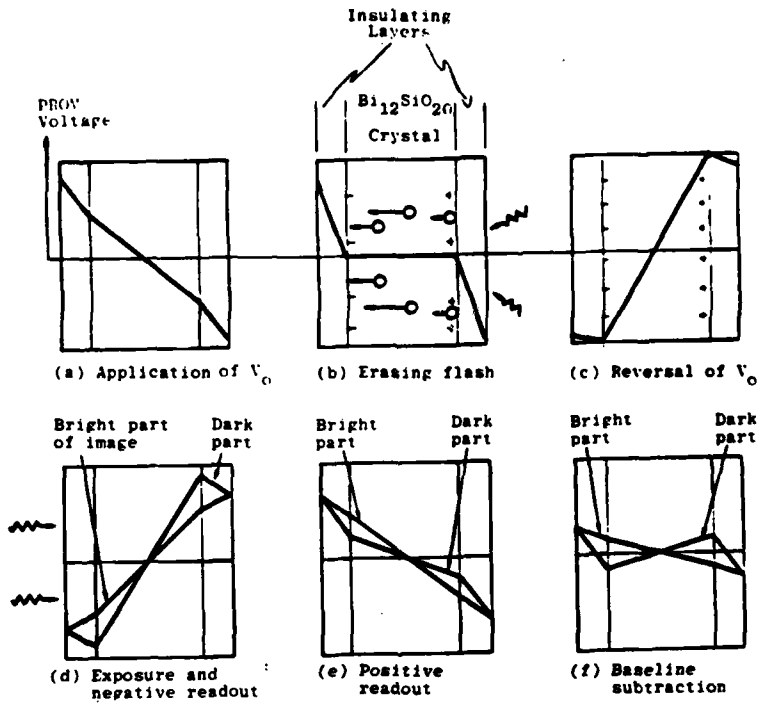

Fig. 3.2 - PROM MTF for Various Exposures Measured by Diffraction Techniques

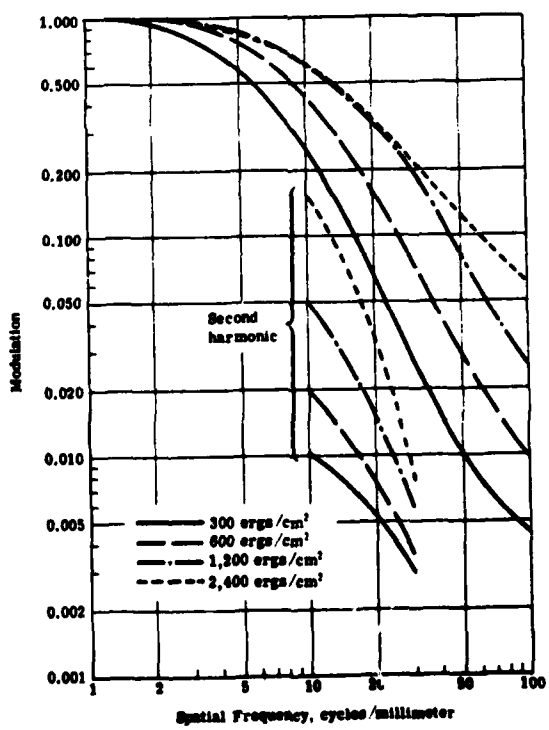

4. ANALYSIS PROCEDURES AND RESULTS

Upon completion of the two primary analysis tasks, i.e., Filtering Technique and PROM Readout, the PCOP optical schematic was developed. This schematic is shown in Figure 4.1. It accurately represents the generic processor and will be referred to in the following paragraphs.

4.1 Filtering Technique

To operate on the Fourier spectrum of the imagery, a filter is created on the second PROM through exposure by the PROM Laser Scanner. This filter is presently an intensity pattern created to selectively block part of the spectrum in a fashion chosen and controlled interactively. Interactive operation requires a relatively rapid change of the filter with respect to the spectrum. This filter change can take place in either of two ways: writing of an entirely new filter; or a rotation of the existing filter or the image about the system optical axis.

Fig. 4.1 - PROM Coherent Optical Processor Schematic

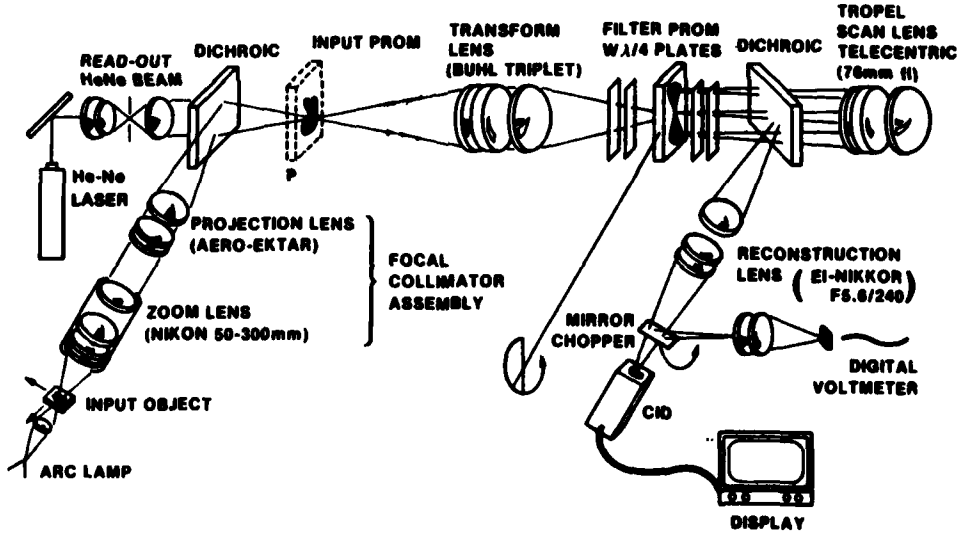

4.1.1 K-Mirror Rotation

In the initial PCOP design concept, a K-Mirror was used to effect rotation of the image with respect to the filter. Operational requirements dictated that the K-Mirror be placed in the transform beam rather than the input imaging system so that continuous rotation rather than rotation synchronized to PROM exposure could be performed. Further analysis showed, however, that this approach gives rise to several difficulties.

The first problem results from the linear polarization of the HeNe laser beam in the Fourier Transform system. In a well aligned K-Mirror, the normals to the 3 mirrors all lie in a plane, the plane of incidence (See Figure 4.2). Linearly polarized light passing through the "K" mirror with a polarization vector either parallel to or perpendicular to the plane of incidence will not suffer any change in state of polarization. For an input polarization vector at an angle θ to the plane of incidence; however, differential phase changes between the polarization components parallel and perpendicular to the plane of incidence will result in elliptically polarized light at the output of the K-Mirror. Since conventional PROM readout relies upon linearly polarized light, this state of affairs would result in unacceptable intensity modulations as the K-Mirror was rotated.

The phase shift is, in principle, calculable from models of metallic film and dielectric film sandwiches*, but the calculations are quite involved and not necessarily accurate, owing to uncertainties in mirror composition for the actual device we have to work with. The best approach to characterizing an individual K-mirror's properties is through measurement.

Babinet compensator measurements on actual K-Mirrors, both at USAETL and Itek, indicate differential phase shifts on the order of 70^{o} to 95^{o} for these devices. A specially made phase retarder rotating with a given K-Mirror can, in principle, compensate for this effect and produce linearly polarized light out; however, mirror misalignments and the finite input cone likely would have made compensation less than 100% effective. In addition, the K-Mirror/compensator assembly would insert five surfaces into a coherent optical path.

The most bothersome aspect of a rotating K-Mirror, however, is the prospect of a rotating image at the reconstructed image plane. Compensating derotation could be implemented, either by adding another K-Mirror or by a software rotation algorithm applied to the digital image detected by the CID camera. These approaches have drawbacks both in terms of system cost, complexity and speed.

4.1.2 Fourier Plane Filter PROM Rotation

The problems inherent in the K-Mirror approach forced investigation of the possibility of rotating the filter PROM. An analytical investigation of this problem, using the Jones calculus for polarized light beams, indicated that the inclusion of two properly oriented $\lambda/4$ plates between the customary polarizer analyzer pair results in an output intensity that only depends upon the PROM's anisotropic phase retardance, δ, and not on its orientation. A comparison of the conventional and rotating PROM readout systems is shown in Figure 4.3. In the rotating PROM system, the $\lambda/4$ plate axes are oriented at 45^{o} with respect to

*See, for example, Sections 13.2 and 13.4 in Principles of Optics, Third Edition M. Born and E. Wolf, Pergamon, N.Y. (1965).

Fig. 4.2 - Problems of Polarization and PROM Readout
Associated with a K-Rotator

Linearly polarized light undergoes a cumulative phase change upon reflection from the 3 mirror surfaces and becomes elliptically polarized upon K-rotation.

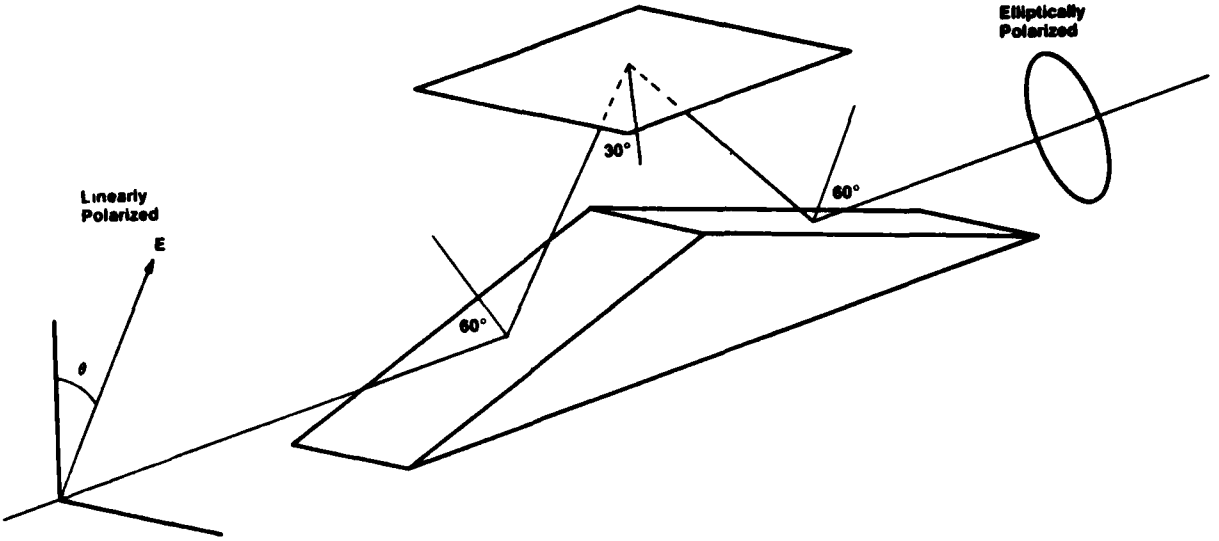

Fig. 4.3 - PROM Readout

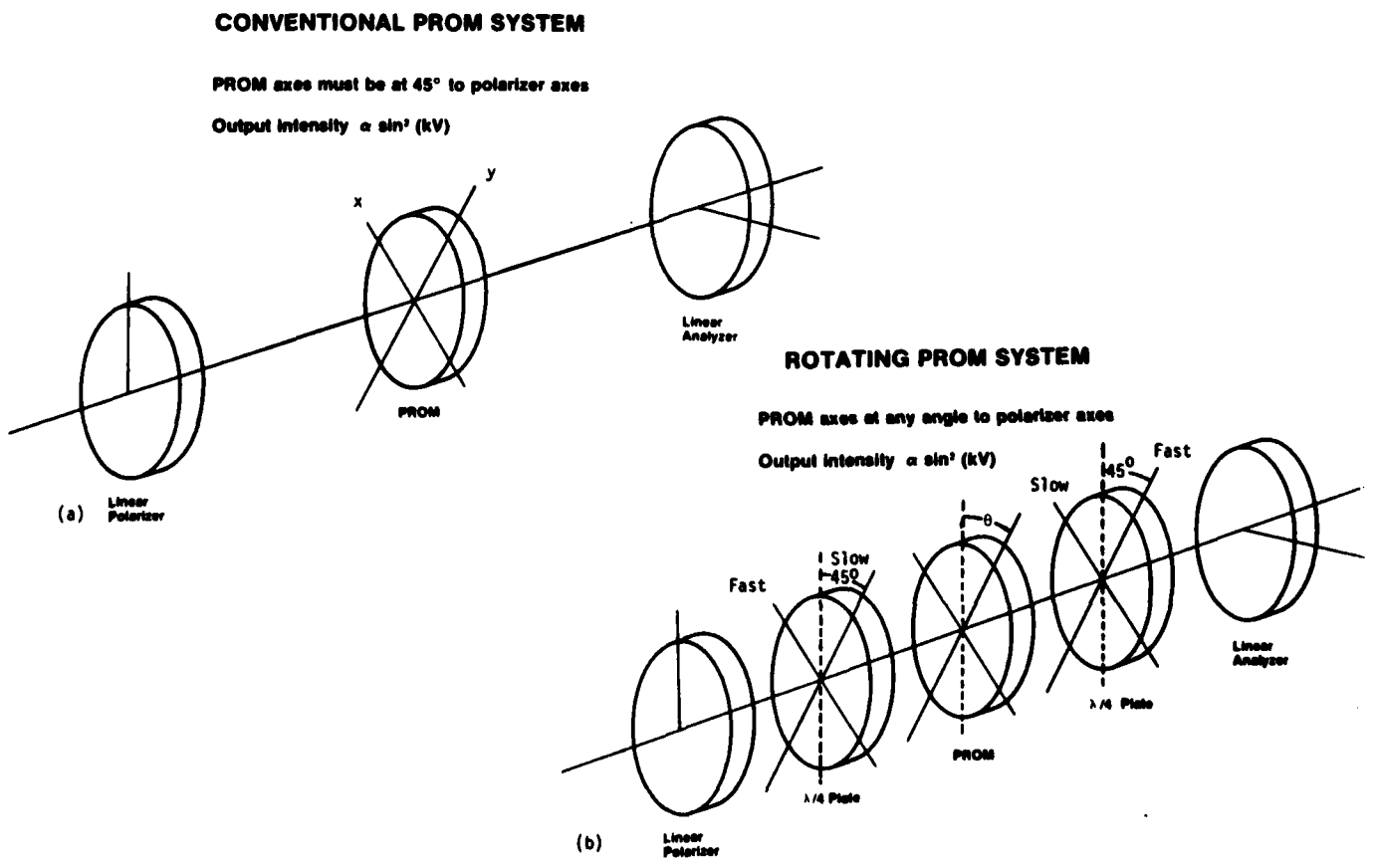

the polarizer/analyzer axes, as shown in Figure 4.3(b). For this configuration, the functional relationship between the output intensity and the PROM voltage has the same $\sin^2(kV)$ relationship as the conventional PROM readout.

For perfect $\lambda/4$ plates, the configuration of Figure 4.3(b) is one of many possibilities: The others result from arbitrary rotations of the second $\lambda/4$ plate and linear analyzer as a unit about the system axis. For $\lambda/4$ plates that are not perfect, however, further analysis reveals that maximum extinction can be obtained by proper orientation of the second $\lambda/4$ plate-analyzer pair with respect to the first pair. Jones matrix calculations covering the conventional and rotating PROM configurations, as well as the case for imperfect $\lambda/4$ plates, are found in Appendix 1.

Experiments were performed to verify the validity of the rotating PROM concept. In one experiment, a 3 bar resolution target was imaged on a PROM. Limiting resolution and image contrast were observed to remain constant as the PROM was rotated through 180°. In a more quantitative experiment, a PROM was uniformly exposed, and the throughput intensity of a HeNe laser beam was measured as the PROM was rotated through 135°. For the probe laser beam directed along the rotation axis of the PROM, throughput intensity varied by less than $\pm$ 5% as the PROM was rotated. The probe beam was then displaced 5 mm from the rotation axis, and variations of less than $\pm$ 10% in intensity were observed. We were unable to perform these experiments with the USAETL PROM which is back for refurbishment, since one of the contacts had lifted from the PROM surface. However, a comparison of the extinctions achieved by placing the USAETL PROM and the experimental PROM between a circular polarizer and analyzer pair revealed no major differences in the two PROM's.

Table 4.1 provides a summary of the advantages and disadvantages associated with the various possibilities for rotation of the Fourier Transform with respect to the filter. The rotating filter PROM concept avoids the problem of image rotation, and is attractive because of its relative electro-mechancial simplicity. However, the fact that the PROM has a wedge angle (to avoid coherent readout problems) introduces a wobble of the reconstructed image about the optical axis, which can be corrected by insertion of a compensating wedge rotating with the PROM. In summary, the rotating PROM mode has been shown to be a suitable method for Fourier Transform/filter rotation within the PCOP system.

4.2 PROM Readout

A PROM may be read out in either reflection or transmission. Readout in reflection appears attractive for two reasons:

1) Cancellation of the crystal optical activity and

2) Doubling of the effective interaction length in the crystal.

While these advantages made reflection the preferred readout mode for early PROM's, recent developments have changed this. The desire to produce more sensitive PROM's has led to thinner PROM crystals, and a consequent difficulty in maintaining surface flatness. The polishing process produces an excellent transmitted wavefront, but a highly aberrated wavefront on reflection.

TABLE 4.1

PCOP Rotation Options

"K" Rotator

Rotate Image

Advantages

- No polarization problem
- Fourier transform rotates without wobble

Disadvantages

- Rotation in discrete steps for PROM exposure
- CID camera image will rotate unless derotation is incorporated
- Stops on "K" limit rotation to < 360^{o}

Rotate Fourier Transform

Advantages

- Rotation can be continuous

Disadvantages

- Fourier transform axis will wobble $\pm$ 130 μm for 1 minute "K" deviation
- Polarization effects will modulate intensity through filter unless compensated. Compensation may be difficult
- CID image rotates unless derotated
- Additional components in coherent system
- Alignment difficult to perform and Maintain

Filter PROM Rotation

Advantages

- Filter, Fourier transform and rotation axes can all be aligned
- No polarization problem
- $\pm$ 5% throughput intensity variations for 180^{o} rotation achieved
- CID image translates but does not rotate

Disadvantages

- Additional Components in Coherent System
- Filter Rotation Limited to $\pm$ 90^{o} unless slip rings for HV incorporated

Figure 4.4 shows interferograms for reflection and transmission readout of the USAETL PROM. Analysis of these two interferograms shows a .2λ rms wavefront error for transmission readout and a .5λ error for reflection readout. This PROM was manufactured several years ago (1973). The PCOP will use it and a new one to be produced in the near future. A PROM built and delivered in 1977-78 is shown in Figure 4.4b. We believe it to be typical of the newer PROM's and it shows that transmission is clearly the preferred readout mode, since better than λ/10 wavefront quality was achieved. A determination of which PROM will be used in the image and filter positions should be made after both PROM's have been evaluated and compared. It is recommended that the new PROM have a wedge on it similar to or greater than the old one to facilitate coherent use.

Fig. 4.4 - PROM Readout

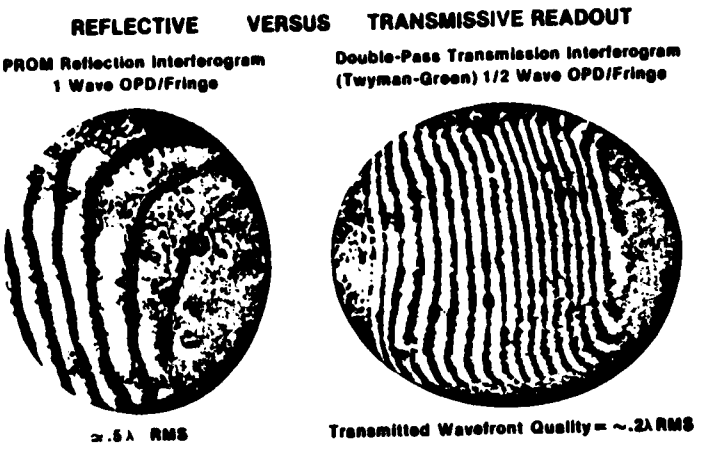

A) USAETL PROM

B) Newer PROM

Transmitted Wavefront Quality =
λ/2>P to P>λ/3
λ/10>RMS>λ/14

4.2.1 Scan Lens Evaluation

PROM Transmission readout led to a requirement for a new scan lens in the PROM laser scanner. This lens was defined through several discussions with USAETL and Tropel, the lens manufacturer. Its characteristics are:

- 76.5 mm focal length
- Scan Angle = $\pm$ 20^{o} (double what is needed)
- Telecentric design
- Back focus = 105 mm
- Corrected for λ = 442 nm

USAETL confirmed that the PLS spot-positioning accuracy was acceptable using this lens. Itek defined the scan lens parameters to make the readout optics compatible with the above lens dimensions and performed analysis to insure that the spot quality was acceptable. This lens is shown in Figure 4.1 and also in the layout drawing referenced in Section 2 (198067).

4.2.2 Dichroic Beamsplitter Analysis

PROM transmission readout requires a dichroic beamsplitter between the filter PROM and the PLS scan lens. The quality of the reconstructed image is not affected by the dichroic beamsplitter to any significant degree because this image is reflected by it. However, its effect on the PROM Laser Scanner focused spot, which forms the Fourier filter, was addressed because this beam passes through the dichroic. A wavefront analysis which considered all the aberations present for the case of a F/25 converging beam passing through a parallel plate .38" thick at 45^{o} to the beam was performed. The PLS lens is telecentric, thus insuring that the analysis performed at 45^{o} is valid over the full field. A third order astigmatism evaluation was also performed which complemented the wavefront analysis. The results of the wavefront modeling showed that while the aberrations would increase the spot size, the new spot parameters were compatible with the PLS operation. Specifically, it was shown that the energy encircled by a $\simeq$ 25 μm spot fell from the theoretical 84% to 53%.

While the intended accuracy of construction of the PLS filters allowed for this increase in spot size, the more significant result of this analysis showed that full aberration correction is achieved by the incorporation of a 9' wedge on the dichroic beamsplitter. Thus, the diffraction limited filter forming spot can be produced upon correct orientation of a wedged dichroic in the PLS converging beam. Figures 4.5 and 4.6 show the point spread functions for the dichroic beamsplitter without and with a wedge respectively.

Fig. 4.5 - Point Spread Function Through a .375" Beamsplitter at 45° to a F/25 Converging Beam. λ=442 nm, no wedge correction.

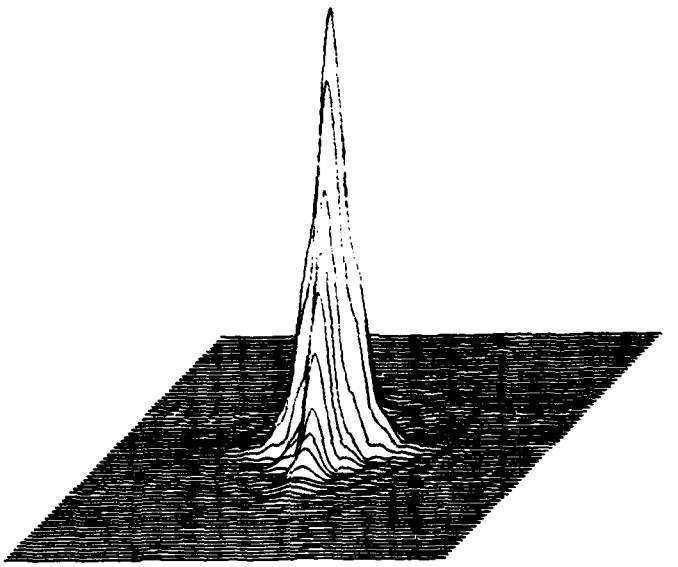

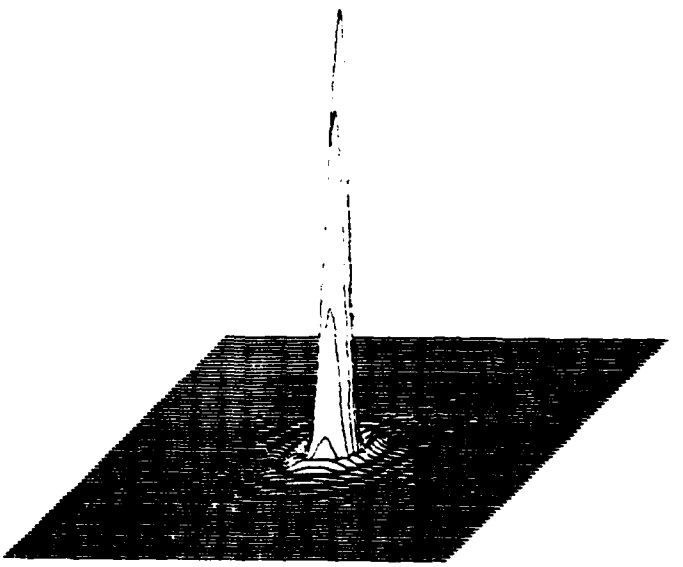

Fig. 4.6 - Point Spread Function for same Conditions as in Figure 4.5, but with a 9' Wedge Correction. Tolerance on wedge correction to maintain near diffraction limited spot is $\pm$ 2'.

4.3 Input Imaging System

This lens system is required to image a transparency on the input PROM with virtually no degradation for conjugates ranging between 1:1 to 1:4, over a maximum image field on the order of 19 to 25 mm. In addition, it is desired that focus holds throughout the zoom range so constant refocusing will not be needed, and that the image will remain essentially stationary on the PROM. Based on typical PROM modulation transfer functions, it is felt that a lens system limiting resolution $\geq$ 100 cycles/mm over the field meets the condition for virtually no degradation.

The purpose of a zoom lens system at the input is two-fold: First, the ultimate goal of this program is to produce a fully interactive Fourier Processor using PROM spatial light modulators. In order to effect this goal, the PCOP optical system was designed to match the spatial frequency range of the input imagery to the modulation transfer function of the PROM. Typical PROM MTF's are shown in Figure 3.2. To provide this match, lens L_1, in the general PCOP schematic of Figure 2.1, was specified to be a zoom optical system operating over the above mentioned magnification range. This insures that the spatial frequency content of areas of interest on the input imagery can be scaled to fall within the region of appreciable PROM response. This operation also effectively changes the transform scale and allows flexibility in filtering the image's Fourier spectrum. Second, the zoom system facilitated selective filtering of imagery, a requirement if relationships between image features and their defining algorithms are to be established.

The zoom focal-collimator arrangement shown in Figure 4.1 was adopted based on previous experience with this type of optical system. A search for a finite conjugate zoom lens, which would have replaced the two lenses with one, was not successful given the time and funding constraints placed on verification of PCOP components. Several tests were made at ETL and Itek before the Nikon - Aero - Ektar performance was found suitable.

With this lens combination, the image was found to move less than 25 microns over the full zoom range, and focus was maintained through the zoom range. Off-axis resolution was good and exceeded the initial goal, as shown in the USAETL report reproduced below.

Finally, object magnification on the PROM varies with the ratio of focal lengths. Thus, object size at the input will range from $\simeq$ 3 mm up to 19 mm or over a range of 1:6 as defined by the two focal lengths, i.e., Nikon fl = 50 - 300 mm, Aero Ektar fl = 300 mm.

USAETL TEST OF ZOOM-NIKKOR W/ AERO/EKTAR

Tangential was worse than sagittal resolution at all field angles. For the on-axis and 6 mm off-axis, the worst tangential resolution was 7-3 at any setting (at 50 mm it is worst). More typically, resolution was 7-5 or 7-6. Sagittal was always 7-6 at all settings.

Shearing interferometer shows good wavefront for zoom from 300 to 100 mm and a sudden onset of coma which then does not change from about 100 to 50 mm f.l. Resolution targets bear out this fact as tangential is degraded relative to sagittal for the shorter focal lengths.

Best zoom imaging is always found when going from shorter to longer focal lengths and all readings were done in this direction.

Best focus for zoom is just opposite the near side lobe of the ∞ sign, i.e., looks like this when viewed from directly above the arrow.

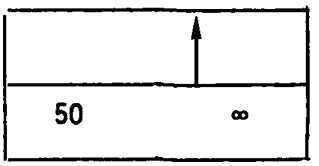

Focus setting arrow

9 mm off-axis

	Focal Length	Sagittal	Tangential
	50+	7-6	7-2
	60	7-6	7-4
	70	7-6	7-5
	85	7-6	7-5
	105	7-6	7-6
	135	7-5	7-5
	200	7-4	7-1 or 7-2
	250	7-2	6-6
about	275	7-2	7-1 (119 cycles/mm)
	300	out of range of translation stage	

4.4 One PROM and Two PROM System Options

A primary requirement for the PCOP is the provision of the capability to bypass the image PROM and transform the input image directly. The transform scale change, which is effected in the two PROM system by conjugate changes in the imaging system, is accomplished here by allowing the input transparency to be moved in the focusing transform beam. The focal plane amplitude distribution at the filter is the Fourier transform of the input with a quadratic phase factor included, with the exception that the scale of the transform is decreased by a factor d/ℓ, where d is the distance from the transparency to the filter plane and ℓ is the transform lens focal length. Therefore, the flexibility of matching the maximum spatial frequency of interest in the original image with the available aperture size of the filter is preserved.

The one PROM system is shown in the layout drawing (198067) of Section 2. Enough room for transparency movement has been provided to allow at a minimum a 3:1 transform scale change. The input object dimensions are also changed by being in the converging beam. A variable aperture has been specified to facilitate this.

It was believed that specification of elaborate drive mechanisms to automatically reset the CID camera as the transparency is moved was premature. Specification of a zoom reconstruction lens (finite conjugate) also was inappropriate considering the previously defined image quality - cost guidelines. Therefore, the one PROM system has been defined as noted in the December Monthly Report, and repositioning of the reconstruction lens and CID camera as shown in drawing 198067 are performed to achieve the desired transform scale - reconstructed image conjugate changes. Sufficient flexibility has been designed to allow these changes. A number of variations in operating mode can be achieved by selective lens - CID positioning. These will be reviewed and used according to desired goals during phase 2.

Appendix 2 contains additional analysis performed to define viable operating modes in the one PROM system. Lens - CID positions are noted for cases of interest.

4.5 Transform - Reconstruction Lens System

The optical engineering, analysis and experimental tasks performed on the PCOP are noted in Figure 2.2. Figure 4.7, a computer generated model of the Transform - Reconstruction lens system, with its operating characteristics also noted, will be referenced in describing the work.

4.5.1 Transform Lens

The transform lens quality must be good enough to allow the input PROM to be positioned over a range of locations out to one focal length before it. In addition, other characteristics required of the lens are: a bandpass cutoff larger than the image processing requirement, a long back focus, a flat focal plane, minimum number of surfaces, and suitable image quality in the reconstructed image. Imaging lenses and specially designed "Fourier transform lenses" were eliminated from consideration because their expensive virtues were not needed or actually a hinderance to the concept of a test bed processor. Evaluation focused on a doublet and triplet design. The triplet, naturally, exceeded the doublet performance in image quality at the Fourier plane (flatness) and the reconstructed image plane. Both designs were modeled on the computer, as shown on Figures 4.8 and 4.9, and the results are shown in Table 4.2. The triplet was selected on a combination of cost and performance. As noted in the Table, versatility in selection of input object position is retained with it. A triplet was procured and tested in the Coherent Imaging experiment described in Section 4.5.5.

Its focal length of ~355 mm was defined by the desired upper frequency cutoff of 40 to 50 cycles/mm and by the filter PROM aperture, i.e., 20 mm minimum. These two characteristics essentially fixed the transform reconstruction system dimensions. The input object position was nominally fixed at several inches before the transform lens even though use of the triplet permitted this position to be moved further away from the transform lens.

Fig. 4.7 - PROM Coherent Optical Processor Optical System Analysis

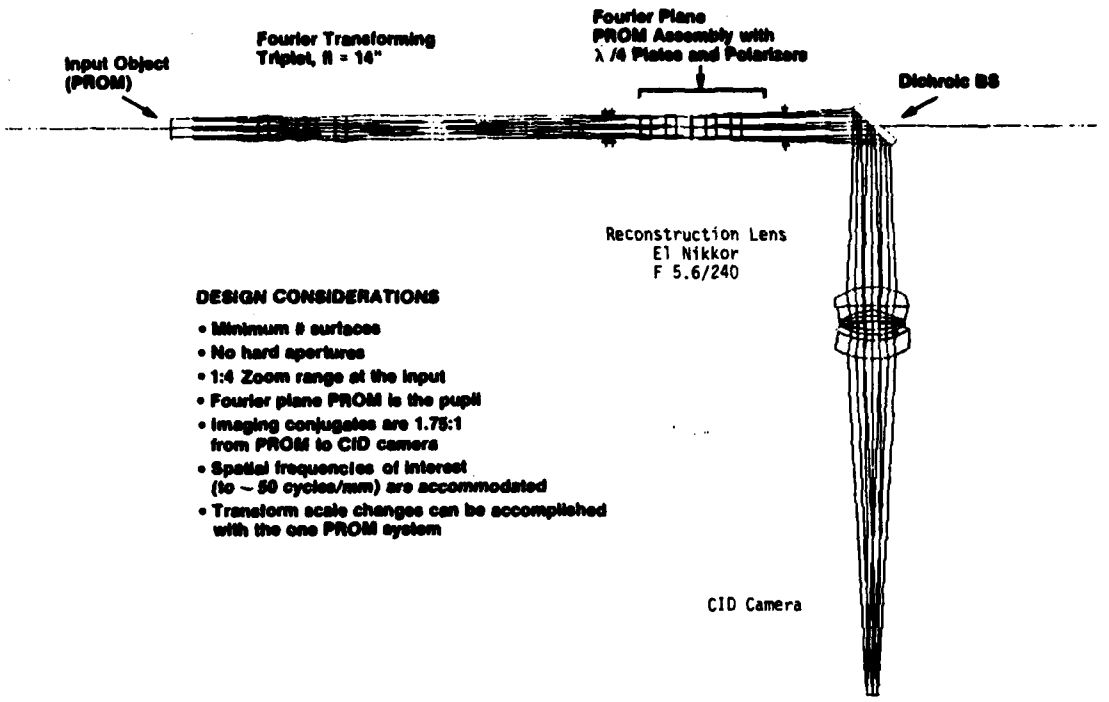

Table 4.2

Fourier Transform Lens Analysis

A. Image Quality at Fourier Plane PROM Surface

	Triplet Design		Doublet Design	
Half-field	Focus	RMS	Focus	RMS
0.0°	25μ	.01λ	162μ	.1λ
1.48°	5μ	.01λ	80μ	.05λ
2.9°	48μ	.03λ	800μ	.26λ

B. Reconstructed Image Quality

Both the doublet & triplet perform diffraction limited for the object (PROM) in the "field" position. Triplet offers significant versatility in allowing for object movement back to the first transform lens focal plane.

Fig. 4.8 - Doublet Design Example

14 in. EFL

f/14 $\pm$ 2.9^{o}

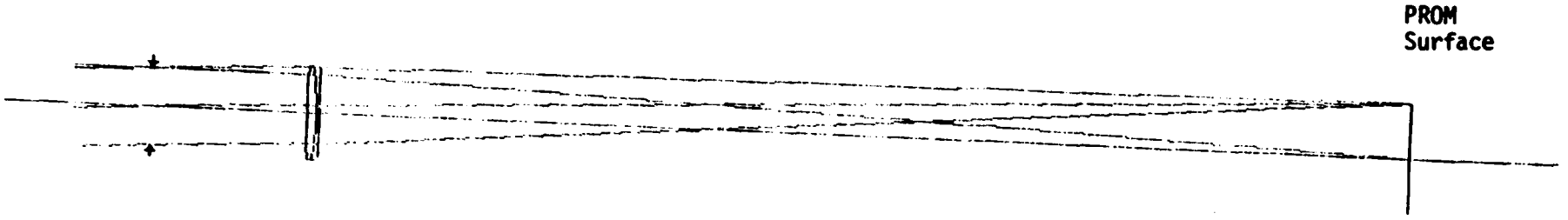

Fig. 4.9 - Triplet Design Example

14 in. EFL

f/14, $\pm$ 2.9^{o}

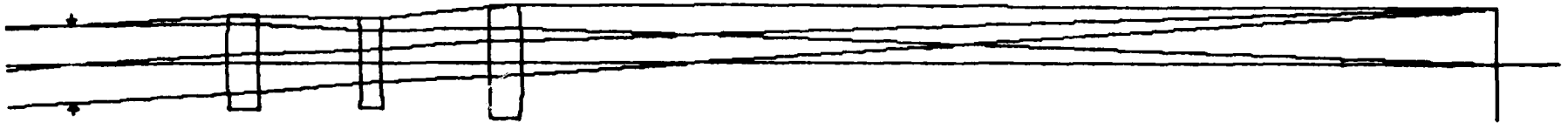

Finally, based on performance in the lab, an off-the-shelf lens rather than a specially designed triplet was specified and is called out in the parts list of Section 2.

4.5.2 Optical Engineering and Conjugate Definition for the Reconstruction Optics

The transform reconstruction lens system was designed to produce a specific transform scale and reconstructed image scale as noted in Figure 4.7. The focal length of the reconstruction lens was restricted to a limited range because the length of the transforming system was fixed, and the dimensions of the input PROM aperture and CID sensor were fixed. Approximately 240 mm was found optimum for the 1.75:1 scale reduction needed to image the input PROM onto the CID sensor.

The F number was required to be fast enough to prevent any low-pass filtering or hard aperture ringing and their undesirable effects on the image. Finally, it was also necessary to have a lens designed for the range of 1:1 to 2:1 imaging conjugates. The optimum for this was an El-Nikkor F/5.6/240 mm fl lens. This lens was virtually the only one found to meet these requirements, and in addition, was attractive because of price and availability. Details of the selection process are discussed in the December report. This lens was procured for the coherent imaging experiment reported in Section 4.5.5.

It was also modeled for the analysis as shown in Figure 4.7. Here, its effect, coupled with that of the transform lens, polarizer and $\lambda/4$ plates, on the reconstructed image was calculated by a wavefront analysis which considered imaging cones whose angles were .5, 1, and 2 times the expected diffracting cone (40 cycles/mm) emanating from the input PROM and traveling through the system to the CID camera plane.

The analysis was performed with incoherent light and because of this the results were chiefly used to illustrate differences between relative variables, i.e., lens system only vs lens and PROM, vs PROM used in reflection and transmission; and to show performance for the on axis vs edge of the field case. Results showed the optical system fully adequate to accommodate the diffracting beam which was limited to $\pm 1.45^{o}$ over a 25 mm input aperture and limited by the aperture of the filter plane PROM. Details of the analysis are discussed in Section 4.5.6.

The optical system, as it is now specified from existing optical components, could be improved upon with a special design made for a coherent reconstruction application. However, this analysis showed the lens quality significantly greater than that with the PROM in the system, so until significant PROM improvements are made, this design is more than sufficient.

4.5.3 Integrated Transform Optics and Sensor

In order to measure the total energy in the transform and compare this value, in a to be determined fashion, with filtering parameters, the chopper mirror, condensing optics and photo diode shown in Figure 4.1 are used. The

chopper mirror will be activated on operator command or automatically, and direct the reconstruction beam through a condensing lens onto a photo diode. The condensing lens focal length (52 mm) and sensor surface area (5 mm diameter) were made to insure that the transform plane is reimaged without vignetting.

The filter diameter of 20 mm is reduced by a factor which varies as a function of the reconstruction lens - Fourier plane distance. Radiometric calculations were also performed to insure that the available energy and the photo diode were matched.

4.5.4 CID/Film Sensors

The primary output of the PCOP is a reconstructed image sensed with a CID camera and displayed on a CRT for operator interaction and feedback CID camera resolution, as determined by the active element dimensions, is equivalent to ≃ 25 cycles/mm. As detailed in Section 4.5.6, the image quality produced at the CID plane is compatible with the camera resolution.

Results from the two PROM system will be in the frequency response range of the CID camera. However, the one PROM system can potentially produce reconstructed imagery at higher spatial frequencies. This may become incompatible with CID response because of aliasing; for this case, if a problem occurs, use of film at the reconstructed image plane could be employed. Imagery output onto film is presently considered to be the secondary operation mode, however, no difficulties with recording the reconstructed image with a film camera back have been found.

4.5.5 Coherent Imaging Experiment

An experiment was conducted to verify the optical quality of the transform-reconstruction system in coherent light. The optics from the transform lens to the reconstruction lens were set up as shown in Figure 4.1 with the exception of the $\lambda/4$ plates and polarizers. A Buhl triplet of focal length = 15.5 inches and a doublet were used as the transform lens and the EL Nikkor F/5.6/240 lens was the reconstruction lens. A continuously increasing frequency grating on film (medium contrast) and an Ealing high contrast target were used as inputs, both with and without a liquid gate to simulate the input PROM imaging. The input was placed just before the transform lens as in the two PROM system. The filter plane PROM was not activated but placed in the system to measure its effect on the output wavefront. The ETL PROM was used here. Imagery conjugates were varied between 1.7-2.0:1. Resolution was measured on axis and out to 12 mm off axis.

Results:

Changes in resolution as a function of axial position and PROM rotation were observed with the doublet transform lens. A coherent system will theoretically produce an MTF of one out to the cutoff frequency. However, the image quality fluctuated as the phase function was varied, but resolution to the cutoff could be maintained by adjusting focus of the viewing device. The phase disturbances or degradations in image quality manifested themselves

by the changing contrast of the targets and coherent noise interference with the imagery. On axis, and with certain PROM orientations, resolution with the doublet was observed to the coherent cutoff of 70-90 cycles/mm in the CID plane. Loss of quality was observed off-axis and as a function of PROM rotation. Resolution here was observed up to 50 to 60 cycle/mm.

A significant improvement in the clarity by reduction in the backbround noise, and sharpness of the imagery, was observed with the triplet transform lens. Here the imagery was less affected by the vagaries of its changing phase function, and resolution near or to the coherent cutoff of 70-90 cycles/mm was observed with relative ease for all PROM orientations both on and off axis.

Figures 4.10a through 4.10c show the reconstructed image of the target at three orientations as it is rotated about the optical axis. The transform taken by the triplet lens passed through the PROM at three different locations which caused detectable variations in image quality as shown in the figures. There was, however, only one orientation, as shown in Figure 4.10c, at which a loss in resolution of one group or approximately 15 cycles/mm, could be detected.

It is possible that local PROM surface anomalies are responsible for the changes in image quality. It may be possible to determine preferred orientations of the filter PROM which will be functions of the other processing parameters, such as frequency, filter shape, etc.; by conducting an experiment similar to this one during the assembly of the PCOP.

Resolution measured with the medium contrast grating, which was more similar in contrast to operational imagery than the target, was found to be 60-65 cycles/mm. The liquid gate reduced the coherent artifacts noticeably.

Reflection readout of the PROM was also simulated. Astigmatism in the image and a significant loss in quality were noticeable for this case. Here, cutoff resolution was lower, in the range of 45-60 cycles/mm, but the coherent disturbances to the phase function made the target almost spurious at about 20 cycles/mm.

Figure 4.11 shows the target in the reconstruction plane and its ghost created by second surface reflection from the PROM. This PROM's wedge angle of 17' - 18' caused a secondary image to appear, whose intensity is approximately .013 of the primary image. This resulted in a modulation of .37 from interference between the two images and produced noise of 2:1 contrast at the outer edges of the image. There is no interference when the input is less than 12 mm diameter.

A PROM, in the Fourier plane, with a wedge angle on the order of 30 to 40 minutes, will eliminate the ghost over the CID image format. A part of the optical design analysis showed that image quality losses due to such a wedge, are negligible. It is also expected that the image wobble, at the reconstruction plane, can be effectively eliminated by using the appropriate compensating wedge rotating with the PROM as described in Section 4.1.

Fig. 4.10 - Reconstructed Target Image

PROM Orientation ~0°;
Resolution~80 cycles/mm

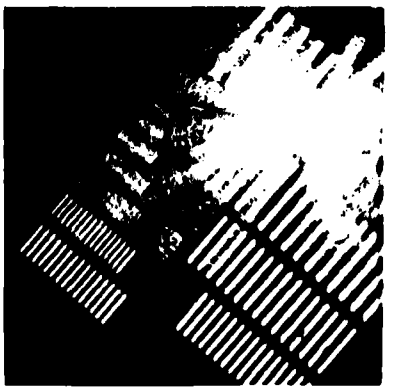

PROM Orientation ~45°;
Resolution~65 cycles/mm

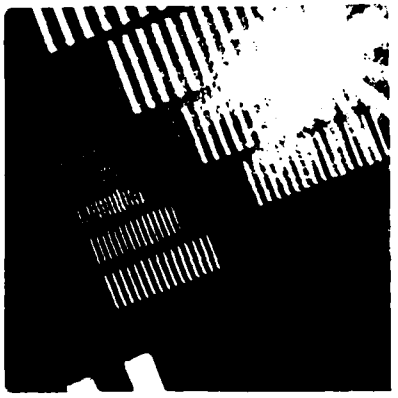

PROM Orientation ~110°;
Resolution~80 cycles/mm

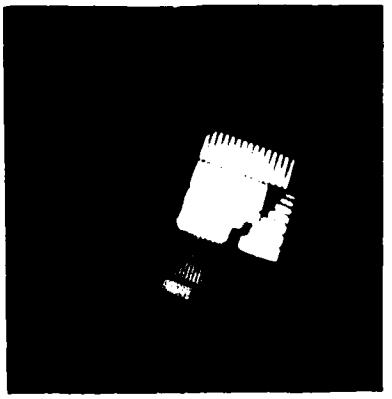

Fig. 4.11 - Reconstructed Target Image

This shows the secondary reflection from the PROM

In summary: optical quality at the reconstruction plane is good with the recommended design. Resolution to the coherent cutoff on and off axis was measured, with minimal coherent anomalies observed over the full field. Noise in the outer third of the image from secondary PROM reflections is unavoidably present. If the noise is found significant in the processing, then the input image size can be reduced or a larger wedge on the filter PROM can be produced.

4.5.6 Image Quality Throughput

A summary of image quality achieved at each step of the processing operation with the PCOP is shown in Figure 2.2. From it we see the following:

The input imaging system, by virtue of its measured resolution cutoff over the desired field produces virtually no effect on the image once the input PROM has been used to record the image. This lens system is used only with this PROM. Its MTF is shown "constructed" from the test data. This MTF cascaded with the PROM modulation transfer sends a relatively low frequency image through the coherent transform-reconstruction system. Here the imagery will be passed with minor observed phase distortion effects to the coherent cut-off of 40 to 50 cycles/mm measured at the object. With the conjugate reduction, output image resolution exceeds the CID resolution. At the CID limit of approximately 25 cycles/mm, image modulation is 40% which is a standard goal in the design of E/O systems. Essentially, the reconstructed image quality is that of the PROM for the two PROM system. Spatial frequencies of interest on the original aerial imagery are adjusted to the range of appreciable PROM response by the zoom input system.

In the one PROM system, output resolution will be governed by the coherent frequency limit designed for the system. The measured limit at the reconstruction plane was 70-90 cycles/mm. This may result in an aliasing problem on the CID. Film used as the output sensor of either the one or two PROM systems will allow full use of the available resolution.

The PCOP optical system was designed to produce a reconstructed image whose quality is determined by the PROM. This is demonstrated by the point spread functions produced by the modeling analysis and shown in Figure 4.12 and Figure 4.13 for (a) the system without the PROM, (b) with PROM readout in transmission and (c) PROM readout in reflection. Figure 4.13 shows the point spread functions for the off-axis edge of the field case.

Finally, this analysis produced a family of MTF's for the system with the PROM in transmission (4.14a) and reflection (4.14b). Changes in visual resolution are illustrated by the MTF's which vary with the PROM rotation angle. Actual resolution values can not be construed from this analysis because of the coherent - incoherent relationship; however, these results are used here to illustrate the fact that optimum PCOP performance will be achieved only through careful alignment, and orientation of all components including the Fourier plane PROM.

4.6 Design Summary for PCOP

This PROM Coherent Optical Processor has been designed to be compatible with the image operations ETL expects to perform and is intended for test bed

c) PROM IN REFLECTION
60μ SPOT DIA. 67% E

b) PROM IN TRANSMISSION
44μ SPOT DIA. 67% E

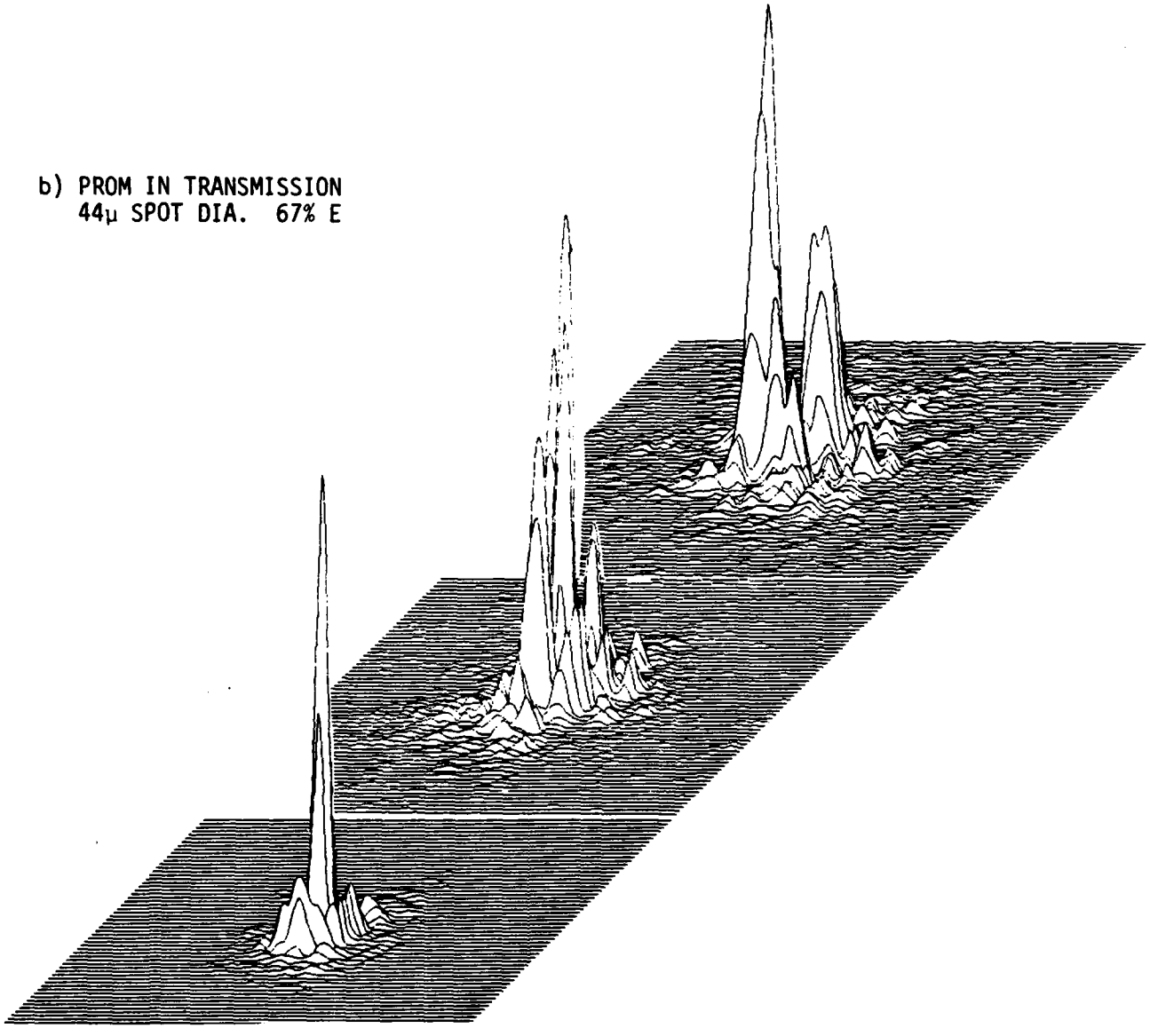

a) NO PROM ERRORS
H = 0.0 28μ SPOT DIA. 67% E

Fig. 4.12 - Point Spread Functions for the PCOP Transform - Reconstruction Lens System from Incoherent Wavefront Analysis, for the On-Axis Condition @ $\pm$ 1.5^{o} cone angle.

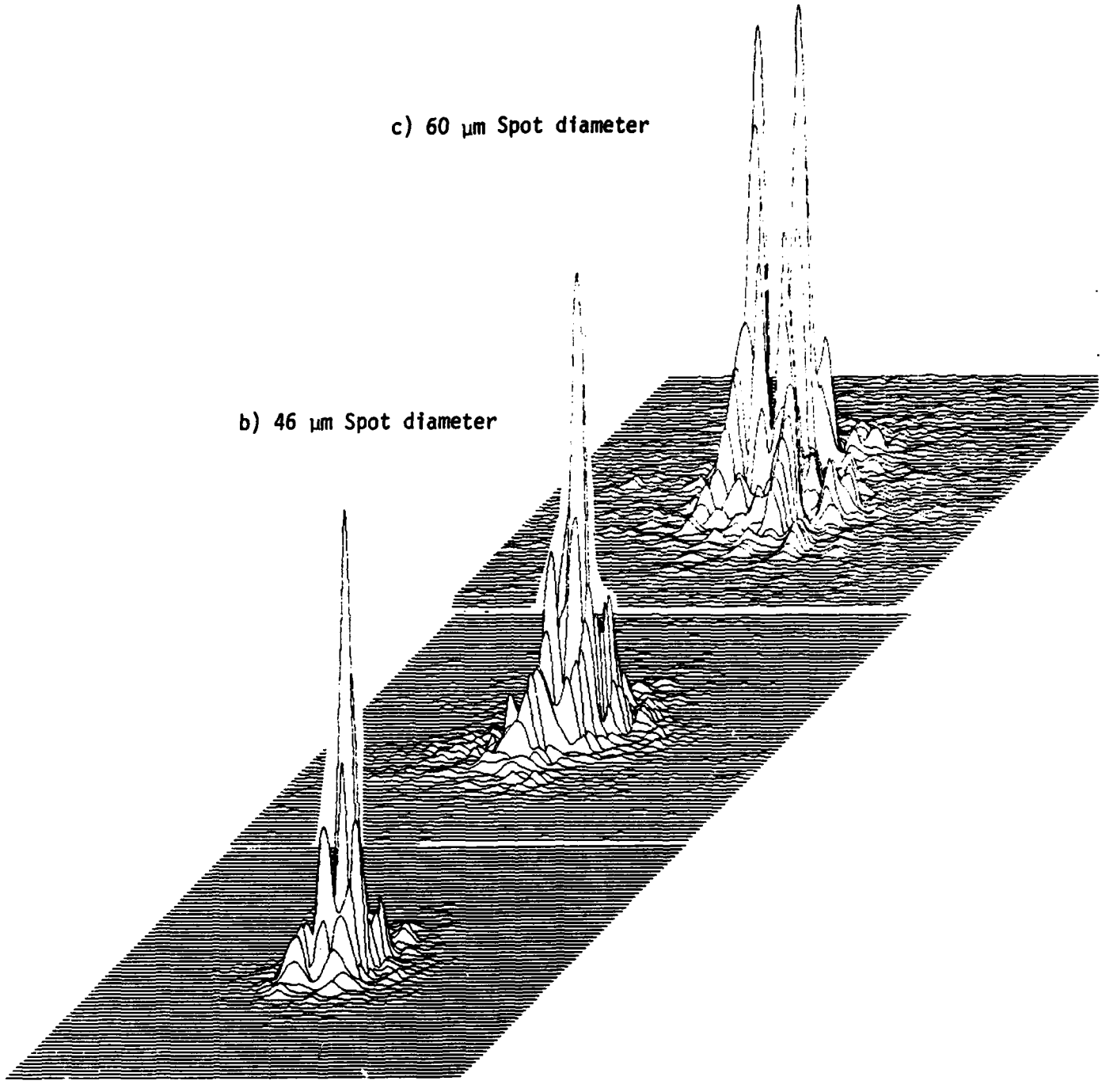

Fig. 4.13 - Point Spread Functions for the PCOP Transform-Reconstruction Lens System @ $\pm$ 1.5^{o} cone angle (a) the edge of the format.

a) No PROM Errors + .11λ Lens mfg. = .17λ RMS
b) PROM in Transmission + .11λ Lens mfg. = .25λ RMS
c) PROM in Reflection + .11λ Lens mfg. = .45λ RMS

Fig. - 4.14(a)

Modulation Transfer Function on Axis
Imaging Cone F/NO = 11.2, Full Field of View 0.0 Degrees
Spectral Range 0.63-0.638
Image Processor PROM in Transmission

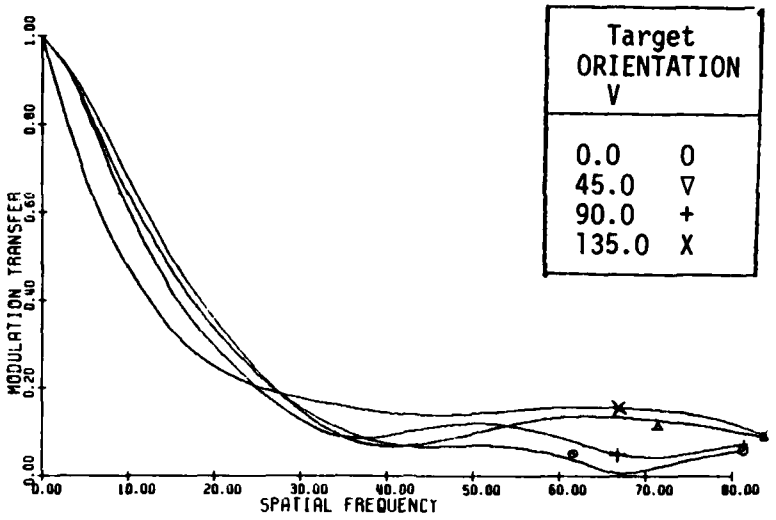

Fig. - 4.14(b)

Modulation Transfer Function on Axis
Imaging Cone F/NO = 11.2, Full Field of View 0.0 Degrees
Spectral Range 0.63-0.638
Image Processor PROM in Reflection

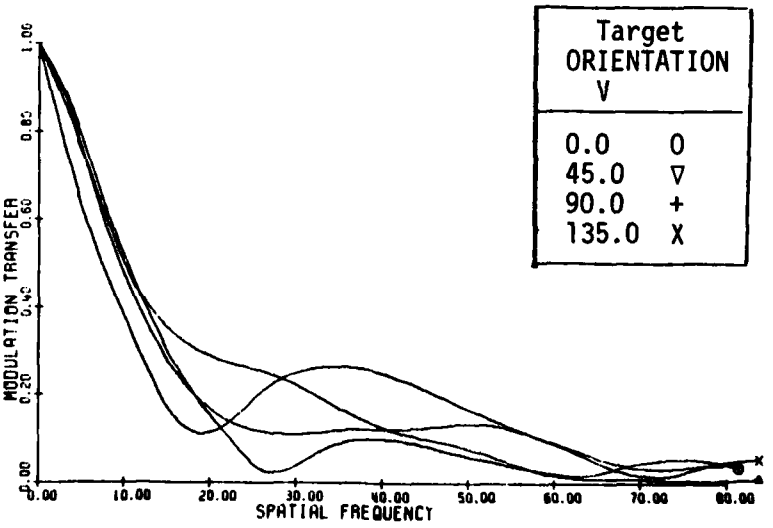

operation. Given the usual course of growth and understanding gained under this type of program, it is possible that desired features and operations will change with PCOP experience. Therefore, one recommended mode of PCOP construction would be to construct fully only those components necessary for concept verification.

The following three steps are intended to serve as a guide for PCOP implementation. (1) The system must be built at the optical quality specified, i.e., the lenses and optical components defined in this study should be used. (2) The Fourier filtering concept developed on the program is required for PCOP operation and therefore the rotating PROM mount and assembly should be built as specified. Sub-assembly test and calibration of the PROM's with processing optics during this state could also be implemented. (3) The other major fabrication assemblies, for example, the lens and input object mounts do not need to be produced immediately. Test bed operations could be begun using laboratory components rather than specially fabricated assemblies. These could be refined and constructed after the image processing/ filtering operations are well defined.

References

1. Horwitz, B.A., Corbett, F.J., Itek Corporation, Optical Systems Division, 10 Maguire Road, Lexington, MA, "The PROM - Theory and Applications for the Pockels Readout Optical Modulator," Optical Engineering, Vol. 17, No. 4, July - August 1978.

2. Nisenson, P., Feinleib, J., Sprague, R.A., Iwasa, S., Itek Corporation, "Characterization and Optimization of an Electro-Optic Imaging Device for Real-Time MAP Profiling," Prepared for: U.S. Army Engineer Topographic Laboratories, Research Institute, Fort Belvoir, VA, October 17, 1974, ETL-CR-74-18, AD-A005 561.

3. Bennett, V., Iwasa, S., Frattarola, J., Spaks, T., Nisenson, P., and Turpin, R., Itek Corporation, "Characterization of the PROM for Coherent Optical Processing Applications," Prepared for: U.S. Army Engineer Topographic Laboratories, Research Institute, Fort Belvoir, VA, August 9, 1976, ETL-0053, AD-A030 137.

4. Shurcliff, W.A., Polarized Light - Production and Use, Harvard University Press, Cambridge, MA (1966).

Appendix 1

PROM Readout Calculations

This appendix provides a sketch of the calculations which were used to compare the conventional and rotating modes of PROM readout. In addition, some calculations involving imperfect $\lambda/4$ plates are given, as well as the resulting conclusions.

These calculations all are framed in the formalism of the Jones calculus for polarized light. This matrix approach is explained in many modern optics texts. The book by W. Shurcliff, Polarized Light[4], has an extensive treatment, together with a comprehensive table of matrices for various polarized light operations.

A.1.1 Conventional PROM Readout

This situation is sketched in Figure 4.3(a). It consists of a crossed linear polarizer-analyzer pair. The PROM is modeled as a retarding plate with its axes oriented at 45° to the axes established by the polarizer-analyzer pair. For the purposes of this calculation, it is assumed to have a phase retardance of δ; that is, light polarized along one axis will be advanced or retarded by a phase angle δ with respect to light of the same frequency polarized along the other axis. For a PROM with an image stored as a charge pattern, δ varies as a function of position on the PROM surface.

The Electric Field amplitude vector at the output of the analyzer is given by the following multiplication of matrix operators. A unit intensity input beam is assumed.

$$\underbrace{\begin{bmatrix} E_x \\ E_y \end{bmatrix}}_{\text{output vector}} = \tfrac{1}{2} \underbrace{\begin{bmatrix} 1 & -1 \\ -1 & 1 \end{bmatrix}}_{\substack{\text{analyzer} \\ \text{at } -45^\circ \\ \text{to x axis}}} \cdot \underbrace{\begin{bmatrix} e^{i\delta/2} & 0 \\ 0 & e^{-i\delta/2} \end{bmatrix}}_{\substack{\text{Phase Plate} \\ \text{with phase} \\ \text{shift } \delta \text{ between} \\ \text{x and y axis}}} \cdot \underbrace{\frac{1}{\sqrt{2}} \begin{bmatrix} 1 \\ 1 \end{bmatrix}}_{\substack{\text{Vector for light} \\ \text{polarized at } 45^\circ \\ \text{to x axis}}}$$

Upon completing the multiplications, we obtain:

$$\begin{bmatrix} E_x \\ E_y \end{bmatrix} = \frac{1}{2\sqrt{2}} \begin{bmatrix} e^{i\delta/2} - e^{-i\delta/2} \\ -e^{i\delta/2} + e^{-i\delta/2} \end{bmatrix} = \frac{1}{\sqrt{2}} \begin{bmatrix} i \sin \delta/2 \\ -i \sin \delta/2 \end{bmatrix}$$

The output intensity is given by $I = E_x E_x^* + E_y E_y^*$, where * denotes complex conjugation.

For this case,

$$(A1) \qquad I = \sin^2 (\delta/2)$$

for conventional PROM Readout

A.1.2 Rotating PROM Readout

A number of configurations which would permit PROM readout for arbitrary rotations of the PROM about the system axis were investigated. The final configuration, shown in Figure 4.2(b), preserves the functional dependence of intensity on δ given by Eq. (A1) for any rotation angle. For this case, the matrices to be multiplied are:

$$\underbrace{\begin{bmatrix} E_x \\ E_y \end{bmatrix}}_{\text{output vector}} = \frac{1}{2} \underbrace{\begin{bmatrix} 1 & -1 \\ -1 & 1 \end{bmatrix}}_{\text{analyzer}} \underbrace{\begin{bmatrix} e^{-i\pi/4} & 0 \\ 0 & e^{i\pi/4} \end{bmatrix}}_{\lambda/4 \text{ plate}}$$

$$\underbrace{\begin{bmatrix} \cos\theta & -\sin\theta \\ +\sin\theta & \cos\theta \end{bmatrix}}_{\text{derotation matrix}} \underbrace{\begin{bmatrix} e^{i\delta/2} & 0 \\ 0 & e^{-i\delta/2} \end{bmatrix}}_{\substack{\text{phase plate} \\ \text{with phase} \\ \text{shift } \delta}} \underbrace{\begin{bmatrix} \cos\theta & \sin\theta \\ -\sin\theta & \cos\theta \end{bmatrix}}_{\substack{\text{rotation} \\ \text{matrix}}} \cdot \underbrace{\begin{bmatrix} e^{i\pi/2} \\ 1 \end{bmatrix}}_{\substack{\text{circularly} \\ \text{polarized light} \\ \text{from } \lambda/4 \text{ \& plate} \\ \text{polarizer}}}$$

PROM with phase shift δ, at any angle θ to x axis.

This string of operators represents the situation of Figure 4.2(b). It results in a zero output vector for all θ if $\delta = 0$. This is easily verified since the PROM operator reduces to the identity matrix in this case.

The more general case, $\delta \neq 0$, while straightforward, is unfortunately a bit more messy. The output electric field vector is

$$\begin{bmatrix} E_x \\ E_y \end{bmatrix} = \frac{e^{i\pi/4}}{\sqrt{2}} \sin(\delta/2) \begin{bmatrix} i\cos 2\theta + \sin 2\theta \\ -i\cos 2\theta - \sin 2\theta \end{bmatrix}$$

and the output intensity is:

$$I = E_x E_x^* + E_y E_y^* = \frac{\sin^2(\delta/2)}{2} \left[2\cos^2 2\theta + 2\sin^2 2\theta\right]$$

Thus, $I = \sin^2(\delta/2)$, the same result as in the conventional case, independent of θ.

The above relationship can also be demonstrated to hold for a more general case in which the final $\lambda/4$ plate-analyzer combination is rotated as a unit about the system axis.

A.1.3. Imperfect $\lambda/4$ Plates

The system of Section A.1.2 assumed $\lambda/4$ plates that produced a perfect quarter-wave phase difference for a 633 nm wavelength HeNe readout beam. As such, the system should work well irrespective of the orientation of the final $\lambda/4$ plate-analyzer combination. Since real systems seldom are built with perfect components, it is worthwhile to ask what effect this might have.

In order to simplify the problem, the approach taken considered only a polarizer - $\lambda/4$ plate and $\lambda/4$ plate-analyzer configuration, with the intervening PROM removed. In addition, since we are considering small deviations from perfection, the system of Figure 4.3(b) (without PROM) was taken as a starting point. That is, the $\lambda/4$ plates were oriented with their fast and slow axes at 45^o to the axes of the polarizers in a manner to produce right and left hand circular polarizers. The second pair, however, is allowed to make an arbitrary angle θ with respect to the x and y axes. The goal is to find the position for minimum throughput intensity.

The concatenation of operators for this situation is as follows:

$$\begin{bmatrix} E_x \\ E_y \end{bmatrix} = \underbrace{\begin{bmatrix} \cos\theta & -\sin\theta \\ \sin\theta & \cos\theta \end{bmatrix}}_{\text{derotation matrix}} \cdot \underbrace{\frac{1}{2}\begin{bmatrix} 1 & 1 \\ 1 & 1 \end{bmatrix}}_{\text{analyzer at } 45^0} \cdot \underbrace{\begin{bmatrix} e^{i(\pi/4+\beta)} & 0 \\ 0 & e^{-i(\pi/4+\beta)} \end{bmatrix}}_{\lambda/4 \text{ plate at } 0^0 \text{ with error } 2\beta} \cdot \underbrace{\begin{bmatrix} \cos\theta & \sin\theta \\ -\sin\theta & \cos\theta \end{bmatrix}}_{\text{rotation matrix}}$$

$\lambda/4$ plate-analyzer combination at angle θ

$$\cdot \underbrace{\begin{bmatrix} e^{i(\pi/4+\alpha)} & \\ 0 & e^{-i(\pi/4+\alpha)} \end{bmatrix}}_{\lambda/4 \text{ plate at } 0^0 \text{ with error } 2\alpha} \cdot \underbrace{\frac{1}{\sqrt{2}}\begin{bmatrix} 1 \\ 1 \end{bmatrix}}_{\text{linear polarized light-polarized at } 45^0}$$

The multiplications in this case are rather tedious. The final result for the throughput intensity in this case is:

$$\text{(A 2)} \qquad I = \cos^2\theta \sin^2(\alpha+\beta) + \sin^2\theta \sin^2(\alpha-\beta)$$

There are two cases to be considered:

a) α and β are of opposite sign. In this case, $\theta = 0$ is the proper orientation. since all terms in Eq. (A 2) are positive definite, and $\sin^2(\alpha+\beta) < \sin^2(\alpha-\beta)$.

b) α and β are of the same sign. Clearly $\theta = 90^0$ minimizes Eq. (A 2)

Since knowledge of the sign of any errors may be difficult to obtain, the best procedure would be to orient the $\lambda/4$ plates at 45^0 with respect to their paired polarizers, and experimentally determine the proper orientation of these pairs for best extinction.

Appendix 2

Calculations and Trade-Off Considered for the Imaging Conjugates of the One and Two PROM System

This appendix contains data which was used in the definition of imaging conjugates for the PCOP.

The need for this definition came from the requirement to provide a variation in the Fourier transform scale. This was accomplished in the two PROM system by changing the image scale at the input PROM through the zoom lens system. This allowed the Fourier transform scale to be changed with respect to the frequency content of the input imagery, without affecting the reconstruction imaging coordinates. The transform range is defined by the zoom lens range and is 6:1. The reconstruction requirement was to image the input PROM onto the CID camera. This requirement, and the length of the transform - PROM - readout optical path established the reconstruction lens focal length at approximately 240 mm.

The one-PROM system was then accommodated as well as possible within the physical constraints of the primary, two PROM system. Calculations using the thin lens equation:

$$\frac{1}{S} + \frac{1}{S'} = \frac{1}{f}$$

where:

S = object dist

S' = image dist

f = focal length of reconstruction lens

were made. The goal was to define the reconstruction lens and CID camera movements necessary to accomplish the two primary requirements defined above, i.e., a) provide a 3:1 Fourier transform scale change and b) reconstruct the input, which was now the aerial transparency, onto the CID camera, so that the CID format was fully used. Table A1 illustrates the results of the calculations. For both the one and two PROM systems transform scale changes are accommodated. In the one PROM system, this is limited to ~3:1 by the physical constraints. Here, the transparency stage is moved in the transforming beam from the transform lens to the filter plane but the physical bulk of the optics, stage and mounts do not allow travel to produce the 6:1 range accomplished in the two PROM system. The table shows that the (near) constant of the calculations was made to be image size on the CID. In the one-PROM system, the reconstruction lens and the CID are first (row b) simply shifted back 200 mm. This is the distance the object is shifted in going from the two to the one-PROM system. For case c,

the reconstruction lens is moved in toward the Fourier plane 50 mm and about 40 mm more for case d while the CID camera is moved the required distance away from the Fourier plane each time, as shown in the S' column.

In summary, if the two PROM system imaging conjugates are fixed at ~1.75:1, and the transform scale changes are to be performed, then the one PROM system is accommodated with minimal movement of the 240 mm reconstruction lens and CID camera.

Table A1

Lens Parameters for Image Reconstruction

(Refer to Figure A1 for Geometry)

		Input Object Dimension	Transform+ Scale	S*	LP*	S'*	CID Image Dimension	Image Scale Factor
a	Two PROM System	19<——>4 mm (zoom)	1<——>.2	660	0	377	11 mm	1.75:1
b	One PROM System	19 mm	.86	660	200	377	11 mm	1.75:1
c		10 mm	.43	492	150	469	10.5 mm	1.05:1
d		6.5 mm	.30	381	110	674	11 mm	1:1.7

+ Transform scale is taken as 1 at 1:1 imaging from the transparency to PROM
* S= object to reconstruction lens distance, mm.
LP= reconstruction lens coordinate, mm.
S'= CID image to reconstruction lens distance, mm.

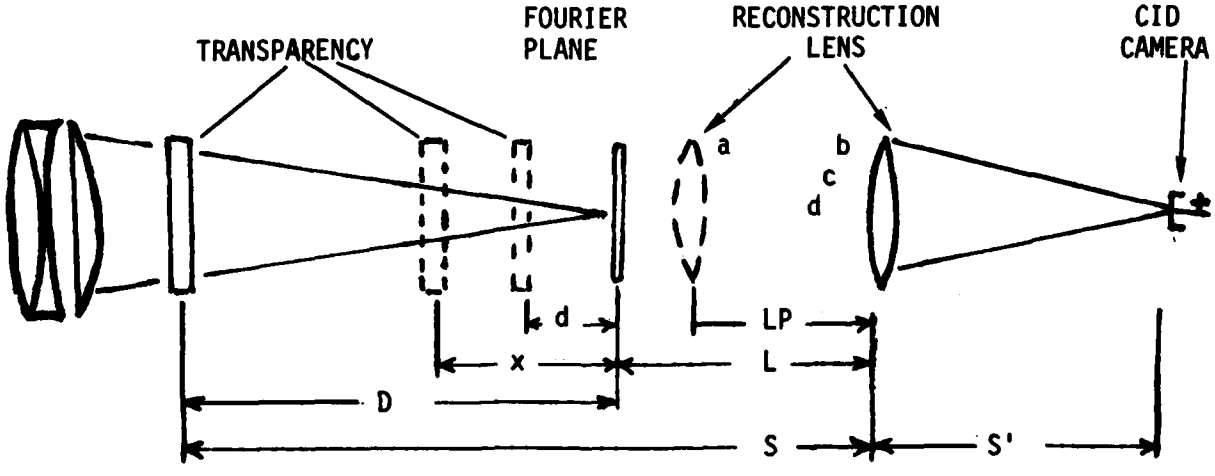

Figure A1

An alternate approach to the one PROM problem considered the possibility of maintaining correct relative change of scale between the Fourier Transform and the CID image by moving only the CID camera.

With reference to Figure A1, we are seeking a fixed reconstruction lens position which is a distance L away from the Fourier plane. Let the input transparency be a distance X away from the Fourier plane, where

$$d \leq X \leq D$$

and

D ≡ maximum distance from the Fourier plane

d ≡ minimum distance from the Fourier plane

The scale of the Fourier Transform when the object is in position X, relative to the scale at D, is given by

$$S = \frac{X}{D}$$

Since there is a reciprocal relationship in scale between Fourier space and Image space, the scale of the image on the CID plane should vary as 1/X.

Consider the imaging equation,

$$\frac{1}{S} + \frac{1}{S'} = \frac{1}{f}$$

In this case, S = L + X, so

$$S' = \frac{f\,(L + X)}{L + X - f} \quad .$$

If we set L = F, this reduces to

$$S' = \frac{f\,(f + X)}{X} \quad .$$

The magnification of the reconstruction system is given by

$$M = -\frac{S'}{S} = -\frac{f}{X} \quad ,$$

thus providing the reciprocal change of scale required.

The focal length of the reconstruction lens will obviously determine the dimensions of the area on the input transparency which will be imaged onto the CID camera. Since a 240 mm lens was selected as optimum for the two PROM system, it is worthwhile to see what its use implies in this mode of operation. The space available for input transparency translation should allow X to range from D = 305 mm to d = 100 mm, for a 3:1 Fourier Transform scale change. The corresponding CID positions will range from 430 mm to 816 mm behind the fixed lens position. The linear dimension covered on the input would be 15 mm when X = 305 mm and 5 mm when X = 100 mm. These dimensions are less than those obtainable by the previous method, in which the reconstruction lens was repositioned. The choice of operational mode can be determined by the user.

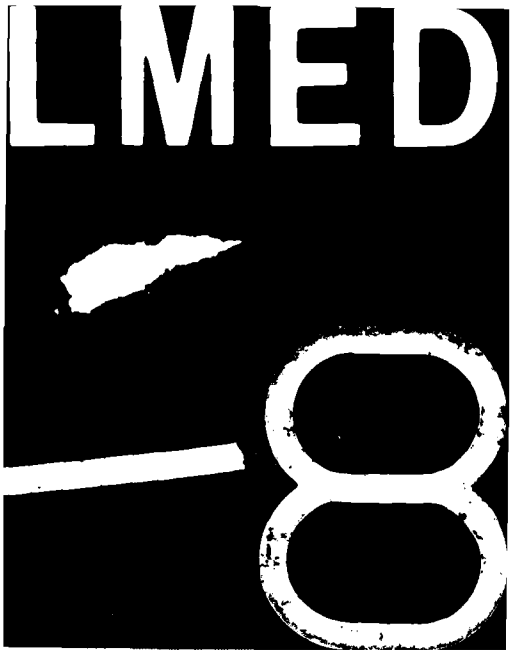
LMED
8